Significance of urea oxidation to nitrite production in the oligotrophic ocean

Xianhui S. Wan[1, 2*], Hua-Xia Sheng[2], Hui Shen[2], Wenbin Zou[2], Jin-Ming Tang[2], Wei Qin[3], Minhan Dai[2], Shuh-Ji Kao[2, 4], Bess B. Ward[1]

[1] Department of Geosciences, Princeton University, NJ 08544, USA.

[2] State Key Laboratory of Marine Environmental Sciences, Xiamen University, Xiamen 361101, China.

[3] School of Biological Sciences, Institute for Environmental Genomics, University of Oklahoma, OK 73019, USA.

[4] State Key Laboratory of Marine Resource Utilization in South China Sea, Hainan University, Haikou, 570208, China.

[*] Correspondence to: xianhuiw@princeton.edu

Key points:

(1) Active urea oxidation in the presence of added ammonium indicates direct urea oxidation by marine ammonia oxidizers.

(2) Substrate affinity regulates the vertical distribution of ammonia, urea, and nitrite in the ocean's interior.

(3) Nitrite production from urea oxidation is comparable to that from ammonia oxidation in the energy-starved mesopelagic ocean.

Abstract

Nitrification, the stepwise oxidization of ammonia to nitrate via nitrite, is a key process in the marine nitrogen cycle. Reported nitrite oxidation rates frequently exceed ammonia oxidation rates below the euphotic zone, raising the fundamental question of whether the two steps are balanced and if alternative sources contribute to nitrite production in the dark ocean. Here we present vertically resolved profiles of ammonia, urea, and nitrite oxidation rates and their kinetic traits extending from the South China Sea to the western North Pacific Subtropical Gyre. Our results show active urea oxidation in the presence of experimental ammonium amendment, indicating direct urea oxidation. Urea oxidation rate covaries with ammonia oxidation rate, and the depth-integrated rates of urea oxidation and ammonia oxidation are comparable, demonstrating urea oxidation is a significant source of nitrite that helps to balance the two steps of nitrification in the oligotrophic ocean. Nitrifiers exhibit high affinity for their substrates, and the apparent half-saturation constants for ammonia and nitrite oxidation decreased with depth. The apparent half-saturation constant for urea oxidation is 1.2 to 11-fold (median 2.2) higher than that for ammonia oxidation at the corresponding depths, but with no clear vertical trend. Such kinetic traits may account for the relatively higher urea concentration compared to ammonium and nitrite concentrations in the ocean's interior. Moreover, combining our results with a review of the previous literature shows a trend of increased urea oxidation relative to ammonia oxidation, from the more eutrophic coastal zone to the oligotrophic open ocean, revealing a substrate-dependent biogeographic distribution of urea oxidation across marine environments.

1. Introduction

Nitrification is a key process of the nitrogen cycle, linking the source and sink of fixed nitrogen, regulating the bioavailability of nitrogen, and contributing to nitrous oxide production and oxygen consumption. In the marine environment, nitrification consists of two steps, the oxidation of ammonia and ammonium (NH_3 and NH_4^+, hereafter referred to as NH_4^+) to nitrite (NO_2^-) by ammonia-oxidizing archaea and bacteria (AOA and AOB), and the oxidation of NO_2^- to nitrate (NO_3^-) by nitrite-oxidizing bacteria (NOB). Ammonia oxidation is generally assumed to be the rate-limiting step owing to the absence of NO_2^- accumulation in the global ocean, with a few exceptions such as the base of the euphotic zone, the oxygen-deficient zone and some eutrophied waters (Casciotti, 2016; Wan et al., 2021; Ward, 2008; Zakem et al., 2018). This idea is supported

by recent measurements showing that the rate of nitrite oxidation outpaces ammonia oxidation below the euphotic zone of the global ocean, despite the significantly higher abundance of AOA than NOB (Santoro et al., 2019; Tang et al., 2023). These observations, however, raise a fundamental question of whether alternative nitrogen sources are required to maintain the high AOA population and sustain the balance of the two nitrification steps in the vast dark ocean.

Mounting evidence from culture and field studies suggests that many AOA and AOB are able to utilize a suite of labile dissolved organic nitrogen (DON) compounds, including urea (Bayer et al., 2016; Carini et al., 2018; Qin et al., 2024), cyanate (Kitzinger et al., 2019; Palatinszky et al., 2015), and polyamine (Damashek et al., 2019) for energy-generating metabolisms, expanding their ecological niche and providing a substantial fraction of NO_2^- for NOB in the NH_4^+-starved environment (Santoro et al., 2019). A recent comparative analysis of available genomes shows that over 50% and 60% of AOA and AOB contain genes encoding urea transport and hydrolysis, suggesting a potentially critical role for urea in sustaining the energy metabolism of ammonia oxidizers (Qin et al., 2024). Urea, which is produced from multiple sources, including organic decomposition, viral lysis, phytoplankton and zooplankton excretion, and human discharge, is a key DON component in the marine environment (Sipler and Bronk, 2015). Notably, urea concentration appears to be higher than NH_4^+ concentration in a variety of open ocean systems, e.g., the Arctic Ocean (Alonso-Sáez et al., 2012; Shiozaki et al., 2021); the Northwestern Pacific (NWP) (Wan et al., 2021); the South China Sea (SCS) (Chen et al., 2015); and the Eastern Tropical North Pacific (Widner et al., 2018). Although urea has long been known as an important nitrogen source for phytoplankton in the oligotrophic ocean (Sipler and Bronk, 2015), its role as an alternative NH_4^+ source for energy production in marine ammonia oxidizers has only been recently appreciated, and quantitative comparisons between urea-derived nitrogen oxidation (hereafter referred to as urea oxidation) and ammonia oxidation in the ocean remain sparse. The relationship between the rates of urea and ammonia oxidation is highly variable in both coastal (Damashek et al., 2019; Kitzinger et al., 2019; J. M. Tang et al., 2022; W. Tang et al., 2022) and open ocean systems (Laperriere et al., 2021; Shiozaki et al., 2021; Tolar et al., 2017; Xu et al., 2019) and is poorly understood.

Another unresolved key issue is whether urea oxidation occurs directly (i.e., urea is taken up and oxidized by ammonia oxidizers) or, indirectly (i.e., urea decomposition by other microbes

provides NH_4^+ for oxidation by the ammonia oxidizers), or both, in the ocean. Although urea utilization by AOA and AOB has been recently studied in various marine systems using different approaches (e.g., ^{14}C labeling incubation, ^{15}N labeling incubation, biomarker genes and their transcription analysis etc.), there is little consensus in the current literature (e.g., Alonso-Sáez et al., 2012; Kitzinger et al., 2019; Santoro et al., 2017; Smith et al., 2016; Tolar et al., 2017). For instance, in the Arctic Ocean and the Central Equatorial Pacific, the significant correlation between archaeal *amoA* and *ureC* gene abundance is interpreted as evidence for potential direct urea oxidation by marine AOA (Alonso-Sáez et al., 2012; Santoro et al., 2017). However, that conclusion is not supported by transcriptional data showing no transcription of *ureC* in the Northeast Pacific (Smith et al., 2016). In the shelf region of the Gulf of Mexico, experiments using urea isotope labeling suggest that over 50% of the measured urea oxidation rate in incubations amended with unlabeled NH_4^+ is attributed to the direct oxidation of urea. However, urea oxidation accounts for only ~7% of the ammonia oxidation rate (Kitzinger et al., 2019). In addition to the inconsistencies reported in prior studies, the fractions of direct and indirect urea oxidation, and how urea oxidation rate responds to addition of NH_4^+ in the oligotrophic open ocean, where the contribution of urea oxidation to NO_2^- production appears to be more important than in the coastal waters, are still unclear. Information on urea oxidation in the oligotrophic ocean thus holds the key to better understanding the source of NO_2^- and the balance of the two steps of nitrification in the ocean.

The kinetic properties of nitrifiers in utilizing their substrates has been widely considered the primary determinant of their competitiveness and ecological niche (Jung et al., 2022; Marten-Habbena et al., 2009). Mounting evidence shows that marine ammonia and nitrite oxidizer natural populations have extremely high affinity (i.e., the measured apparent half saturation constant, hereafter referred as K_s, is at nanomolar level) for NH_4^+ and NO_2^- in the open ocean (e.g., Liu et al., 2023; Peng et al., 2016; Sun et al., 2017; Wan et al., 2018), demonstrating their ability to access substrates at the trace levels at which they occur in the ocean. The kinetic characterization of the ureolytic marine AOA species *Nitrosopumilus piranensis* indicates its higher affinity for NH_4^+ than for urea (Qin et al., 2024). The only available field study on the K_s of urea oxidation reported a range of 146-700 nmol N L^{-1} in the upper euphotic zone of the NWP (Xu et al., 2019). However, there is currently no information available on the kinetics of urea oxidation rate in the mesopelagic ocean, resulting in a knowledge gap about the affinity and energy generation strategy of marine

nitrifiers in the NH_4^+-starved dark ocean. Quantifying and comparing the K_s of ammonia, urea, and nitrite oxidation thus holds the key to enhancing our understanding of marine nitrification homeostatic balance and the distribution of NH_4^+, urea, and NO_2^- in the global ocean.

The subtropical gyres cover nearly 30% of the global ocean surface and are characterized by permanent stratification and oligotrophic conditions. These vast ecosystems play an important role in marine biogeochemistry and are expected to further expand under global warming (Dai et al., 2023; Irwin and Oliver, 2009; Polovina et al., 2008). Despite the extremely low primary productivity and NH_4^+ supply, AOA comprise a major fraction of total prokaryotes below the euphotic zone in the oligotrophic gyres (Karner et al., 2001; Santoro et al., 2019), hinting at alternative substrates for AOA. We hypothesize that urea might play an important role in sustaining the energy generation of AOA to maintain their high abundance in these NH_4^+-starved subtropical gyres. To address these critical knowledge gaps, we investigated the distribution of ammonia, urea, and nitrite oxidation rates extending from the coastal zone of China into the SCS and the western North Pacific Subtropical Gyre (wNPSG). Using the results measured in our study, and by compiling the published data on urea oxidation rates reported in the global ocean, the primary motivations of our study are to: (1) measure the rates and determine kinetic traits of ammonia, urea, and nitrite oxidation across large environmental gradients; (2) characterize the importance of urea oxidation to NO_2^- production; (3) elucidate the spatial pattern of the distribution of urea and ammonia oxidation in the global ocean.

2. Materials and methods

2.1 Sample collection and on-deck incubations

Samples were collected from three research cruises conducted during 2015 to 2021 to the NWP (aboard R/V *Dongfanghong II*), the SCS and the wNPSG (aboard R/V *Tan Kah Kee*). A total of 11 stations extending from the coastal shelf to the open ocean were investigated (Fig. 1a; Table S1), the stations are characterized by a wide range of hydrographic conditions and biological productivity (Wan et al., 2021; Xu et al., 2019). On each cruise, temperature, salinity, depth and fluorescence were measured using a Seabird SBE 911 CTD sensor package equipped with a fluorometer sensor. Discrete seawater samples were collected using twenty-four 12-liter Niskin bottles mounted to the CTD rosette.

Samples for chemical, biological and rate measurements were collected from the same cast. Three 125 mL high-density polyethylene (HDPE) bottles (Nalgene, USA) or 50 mL centrifuge tubes (Fisher Scientific, USA) were used for nutrient collection. Samples for analysis of urea concentrations were collected into acid-washed, precombusted (450ºC for 4 hours) 50 mL amber glass vials. Seawater for isotope labeling incubation was subsampled into 250 mL HDPE bottles. All bottles and equipment were acid-washed and rinsed with *in-situ* seawater at least three times prior to sample collection. Onboard incubations were conducted at four stations across the shelf to the open ocean of the NWP; at three of the stations in the SCS slope and basin and four stations in the wNPSG. Multiple isotope labeling experiments were carried out to quantify ammonia, urea and nitrite oxidation rates. Substrate kinetics for each process were determined at selected stations (Station C3, K6, A8 and B1 in the NWP; Station K11 in the SCS, K8a, MR04 and M30 in the wNPSG) (Table S1). On the 2015 NWP cruise, an additional ^{15}N-L-Glutamic acid (Glu) labeling incubation was performed to compare the oxidation of urea versus amino acid.

For the profile rates of ammonia and urea oxidation, 1 mL of $^{15}N\text{-}NH_4^+$ or ^{15}N-Urea (99% of ^{15}N atom, Cambridge Isotope) and 0.5 mL of $^{14}N\text{-}NO_2^-$ carrier were added to each HDPE incubation bottle with 250 mL seawater to get a final tracer concentration of 20 nmol N L^{-1} and $^{14}N\text{-}NO_2^-$ carrier concentration of 0.5 μmol N L^{-1}. For profile NO_2^- oxidation rates, 1 mL of $^{15}N\text{-}NO_2^-$ (99% of ^{15}N atom, Cambridge Isotope) was added to incubation bottles to get a final concentration of 20 nmol N L^{-1}. For the kinetics experiments, samples from selected depths and stations were incubated at five to six different levels of tracer addition spanning from 10 to 1000 nmol L^{-1} (Table S1). To test whether the measured urea oxidation was direct or indirect, an additional experiment was carried out on the NWP cruise. Specifically, the water samples were amended with four tracer treatments: 100 nmol N L^{-1} of ^{15}N-Urea; 100 nmol N L^{-1} of ^{15}N-Glu (98% of ^{15}N atom, Sigma-Aldrich); 100 nmol N L^{-1} of ^{15}N-Urea plus 2000 nmol N L^{-1} of $^{14}NH_4^+$; and 100 nmol N L^{-1} of ^{15}N-Glu plus 2000 nmol N L^{-1} of $^{14}NH_4^+$. The experiment with unlabeled NH_4^+ enrichment was designed to examine whether the $^{15}NO_2^-$ was produced via direct or indirect oxidation of ^{15}N labeled substrates: If the $^{15}NH_4^+$ from the labeled urea or glutamic acid was produced via heterotrophic degradation, then the $^{15}NO_2^-$ production rate should be decreased substantially (a reduction by 95% because the tracer concentration only accounts for 5% of unlabeled NH_4^+ pool). Otherwise, if the labeled urea or glutamic acid was taken up by AOA, then the decrease in production of $^{15}NO_2^-$ should be less than the predicted 95% decrease. Incubations

were performed with three time points (0, 12, and 24 h). Immediately after injection of tracer and carrier, ~40 mL of sample was filtered through a 0.2 μm syringe filter to preserve for analysis of initial conditions. The remaining samples were kept in a series of temperature-controlled incubators close to *in-situ* temperature (±2℃) in the dark for 12 and 24 hours and were terminated by filtration through 0.2 μm syringe filters. Filtered samples were stored at -20 ℃ after collection. All incubations were implemented in triplicate.

2.2 Sample analysis

NH_4^+ concentrations were measured aboard the research vessel immediately after collection using a fluorometric method with a detection limit of 1.2 nmol N L^{-1} and precision of ±3.5% (Zhu et al., 2013). Seawater samples for quantifying concentrations of other nutrients were stored at -20℃ until measurements in the shore-based lab. Urea concentrations were measured using a liquid waveguide capillary cell based on the colorimetric reaction with diacetyl monoxime with a detection limit of 1 nmol N L^{-1} (Chen et al., 2015). NO_2^- and NO_3^- below the nitracline were measured using a four-channel Continuous Flow Technicon AA3 Auto-Analyzer (Bran-Lube, GmbH), with detection limits of 40 nmol N L^{-1} and 70 nmol N L^{-1}, respectively, and precision better than 1%. Samples with concentrations of NO_3^- and NO_2^- that were near or below the detection limit of the AA3 were analyzed using standard colorimetric methods coupled to a Flow Injection Analysis-Liquid Waveguide Capillary Cell system (World Precision Instruments), with a lower detection limit of 5 nmol N L^{-1} and precision of better than 3% (Zhang et al., 2000).

$\delta^{15}N$ of NO_2^- was measured by chemical conversion (sodium azide, Sigma-Aldrich) of NO_2^- to N_2O (Mcllvin and Altabet, 2005). To determine NO_2^- oxidation rates, the NO_2^- was initially removed from samples by adding sulfamic acid (≥99% sulfamic acid, Sigma-Aldrich) (Granger and Sigman, 2009) and the $\delta^{15}N$ of NO_3^- was determined using the bacterial denitrifier method (Weigand et al., 2016) with minor modifications. Briefly, NO_3^- was quantitatively converted to N_2O using the bacterial strain *Pseudomonas aureofaciens* (ATCC No. 13985), and N_2O was quantified using a Thermo Finnigan Gasbench system (including cryogenic extraction and purification) interfaced to a Delta V^{PLUS} isotopic ratio mass spectrometer (IRMS). $\delta^{15}N$ of NO_2^- values were calibrated against three in-house NO_2^- standards ($\delta^{15}N$ of the three in-house NO_2^- standards were determined using the bacterial method, with values of 0.5 ± 0.4‰, 22.1 ± 0.5‰ and 96.3 ± 0.6‰, respectively). Standard curves were run at the beginning and end of sample

analysis and at ten sample intervals to monitor any instrumental drift and memory effect during the sample measurement. Accuracy (pooled standard deviation) based on analyses of standards at 10 nmol N was ± 0.4‰. $\delta^{15}N$ of NO_3^- values were calibrated against NO_3^- isotope standards USGS 34, IAEA N3 and USGS 32, which were run before, after, and at ten sample intervals. Accuracy (pooled standard deviation) was better than ± 0.3‰ according to analyses of these standards at an injection level of 10 nmol N. For samples with NO_3^- concentrations lower than 0.5 μmol N L^{-1}, 1 mL of 5 μmol N L^{-1} of in-house NO_3^- standard was added as carrier to 9 mL of seawater sample, and the isotopic composition of the sample was then calculated from the measured composition of the mixture and the known in-house standard via mass conservation. The propagated standard deviation was 0.42‰ for these samples (Wan et al., 2018).

2.3 Rate calculation

The reaction rates were determined based on the accumulation of ^{15}N in the product pool relative to the initial (time zero) conditions. To minimize the potential enhancement of the *in-situ* rates due to enrichment by tracer concentrations, the final concentrations of ^{15}N-NH_4^+, ^{15}N-urea and ^{15}N-NO_2^- were limited to 20 nmol L^{-1}. The final concentrations of NH_4^+, urea and NO_2^- in our incubations were close to or lower than the K_s measured in our study and the reported values for ammonia oxidation, urea oxidation and nitrite oxidation rates measured in the wNPSG and the NWP (Liu et al., 2023; Xu et al., 2019), suggesting an overall substrate limiting condition in our incubations. Therefore, we applied a linear regression approach using equations (1-2), with the following assumptions, to obtain the estimates of the *in-situ* reaction rates (Wan et al., 2018).

$$R_{bulk} = \frac{C_t \times n_t - C_0 \times n_0}{t \times f^{15}} \times 24 \qquad (1)$$

$$R_{in-situ} = R_{bulk} \times \frac{Ci_s}{Ci_s + Ct_s} \qquad (2)$$

R_{bulk} is the bulk reaction rate for all substrates after tracer enrichment (nmol N L^{-1} d^{-1}); Ct and C_0 is the product concentration at the ending and beginning of the incubation (nmol N L^{-1}); f^{15} is at% ^{15}N of the substrate pool at the beginning of the incubation; n_t and n_0 are the at% ^{15}N of the product pool at the ending and beginning of the incubation (%), respectively; t is the duration of the incubation (h); $R_{in-situ}$ is the *in-situ* reaction rate calibrated by linear interpolation; and Ci_s and Ct_s are the initial substrate concentration and final tracer concentration, respectively. $R_{in-situ}$ data are the results reported and discussed below. Notably, not all the kinetic tests show a typical

Michaelis-Menten (M-M) type response. Lack of M-M type response has been attributed to trace metal nutrient limitation (Horak et al., 2013) or substrate saturation (Mdutyana et al., 2022b), resulting in uncertainty in using kinetic parameters to calibrate the substrate tracer enrichment effect. Nevertheless, given the general substrate limitation and the low tracer concentration (20 nmol N L^{-1}) we used during the incubation, this method still represents a reliable and widely used approach for deriving the *in-situ* rates in substrate-limited environments.

The depth-integrated (0-1000m) rate was derived using trapezoidal extrapolation of the *in-situ* reaction rate.

The kinetic response of each process was quantified using the M-M equation (3).

$$R_i = \frac{V_{max} \times Cis}{K_s + Cis} \quad (3)$$

R_i is the reaction rate for all substrates after tracer enrichment (nmol N L^{-1} d^{-1}); V_{max} is the potential maximum rate (nmol N L^{-1} d^{-1}); K_s is the half saturation constant (nmol N L^{-1}); Cis is the bulk substrate concentration (i.e., *in-situ* concentration plus tracer addition; nmol N L^{-1}). V_{max} and K_s were derived based on fitting the curve of the equation (3) using the measured conversion rates and the substrate concentrations.

2.4 Detection limits and statistical analysis

The detection limits depend on the concentration of the product pool and the fraction of ^{15}N in the substrate pool during the incubation. The accuracy of $\delta^{15}N\text{-}NO_3^-$ and $\delta^{15}N\text{-}NO_2^-$ isotope composition measurement was better than ±0.3‰ and ±0.4‰ respectively, and we here use 3 times the standard deviation as a minimum enrichment of ^{15}N in each product pool. Therefore, we calculated detection limits of 0.01 to 0.05 nmol N L^{-1} d^{-1}, 0.01 to 0.10 nmol N L^{-1} d^{-1} and 0.01 to 0.90 nmol N L^{-1} d^{-1} for ammonia oxidation, urea oxidation, and nitrite oxidation, respectively. The comparisons of reaction rates and kinetic parameters were examined by using the Student's t-test. A p-value of < 0.05 was considered significant.

2.5 Compilation of ammonia oxidation and urea oxidation rates measured in the ocean

To investigate the spatial pattern of urea oxidation and ammonia oxidation rates and examine the potential environmental controls on the relationship between urea and ammonia oxidation rates,

we compiled the available published data for simultaneous marine urea and ammonia oxidation rate measurements. A total of 187 measurements were collected for analysis, from study areas extending from the coastal ocean (i.e., estuaries, shelf) (Damashek et al., 2019; J. M. Tang et al., 2022; Kitzinger et al., 2019; Tolar et al., 2017; W. Tang et al., 2022; Xu et al., 2019) to the subtropical oligotrophic ocean (Wan et al., 2021; Xu et al., 2019) and the mid- and high-latitude oceans (Damashek et al., 2019; Tolar et al., 2017; Shiozaki et al., 2021). To ensure accurate quantitative rate comparison and rate ratio calculation, rates which fell below the detection limits were not included in the compilation. Moreover, because different ammonia-oxidizing lineages show distinct NH_4^+ and urea preferences (Qin et al., 2024), and taking into account the fundamental control of substrate concentration on nitrifier community structure and activity (e.g., Martens-Habbena et al., 2009; Santoro et al., 2019), we grouped the collected data into three categories, based on distinct urea and NH_4^+ concentrations and ratios, and different ammonia oxidizer community structures: the eutrophic coastal waters (identified as the bottom depth < 200 m); the epipelagic zone in the open ocean (<200 m) where the AOA community is dominated by the Water Column A ecotype; and the mesopelagic ocean (200-1000 m) where the AOA community is dominated by the Water Column B ecotype (Francis et al., 2005; Qin et al., 2020; Santoro et al., 2019).

3. Results

3.1 Hydrography and nitrogen nutrient distributions

The T-S diagram, the potential density anomaly, and fluorescence profiles showed distinct physical properties of the three study areas (Fig. 1b; Fig. S1). The density gradient was highest in the epipelagic layer of the SCS, but was less pronounced in the mesopelagic zone of the SCS compared to the wNPSG due to more intense vertical mixing at the basin scale in the SCS (Zhu et al., 2019). The NWP stations were characterized by the lowest density gradient. The deep chlorophyll maximum (DCM), as indicated by fluorescence, shoaled upward from the subtropical gyre to the mid-latitude zone, accompanied by increased chlorophyll maximum concentration, implying a northward intensification of biomass and primary productivity.

NH_4^+ concentrations were consistently low (i.e., < 20 nmol L^{-1}) at the SCS and the wNPSG stations with a few exceptions of maxima (e.g., ~ 100 nmol L^{-1}) at the base of the euphotic zone

of the SCS stations (Fig. 2a). The depth-integrated NH_4^+ inventory (0-1000 m) ranged from 3.5-8.3 mmol N m^{-2} in the wNPSG, and was 5.2-20.1 mmol N m^{-2} in the SCS (Table 1). Urea concentration showed no clear vertical pattern with two exceptions at the SCS stations (Q40 and A5) (Fig. 2b). Urea concentration (1 to 119 nmol N L^{-1}, median 51.6 nmol N L^{-1}) was higher than the corresponding NH_4^+ concentration (1 to 109 nmol L^{-1}, median 8.0 nmol L^{-1}) at nearly all stations and depths. The depth integrated urea inventory was 44.5-66.1 mmol N m^{-2} in the wNPSG, and was 55.9-73.9 mmol N m^{-2} in the SCS. Therefore, urea inventory was 3.3-11.5-fold greater than the NH_4^+ inventory in SCS, and the ratio increased to 6.6-18.9 in the wNPSG, suggesting an elevated stock of urea relative to NH_4^+ in the more oligotrophic region.

Prominent primary NO_2^- maxima (PNM) were detected at all stations (Fig. 2c). The depth of the NO_2^- maximum was deeper (100 to 140 m) and maximum concentration (86 to 147 nmol L^{-1}) was lower in the wNPSG compared to the SCS (i.e., depth ranged from 70 to 130 m, concentration ranged from 155 to 208 nmol L^{-1}), resulting in a higher depth-integrated NO_2^- inventory (0-1000 m) in the SCS (15.2-25.2 mmol N m^{-2}) compared to the wNPSG (11.7-17.8 mmol N m^{-2}). NO_3^- concentrations remained low in the upper mixed layer at all stations (i.e., < 1 μmol L^{-1}), and the depth of the nitracline (here defined as the first depth with NO_3^- concentration > 1 μmol L^{-1} (Shiozaki et al., 2011)) shoaled upward from the wNPSG to the SCS (Fig. 2d). The depth-integrated NO_3^- inventory was higher in the wNPSG (27.4-43.1 mol N m^{-2}) than in the SCS (15.4-29.5 mol N m^{-2}) (Table 1).

3.2 Ammonia, urea, and nitrite oxidation rate profiles

Ammonia and urea oxidation rate depth profiles (0-1000 m) were measured at seven stations in the SCS and the wNPSG, and nitrite oxidation rate was quantified at five stations in the wNPSG. All the profiles demonstrated a similar vertical pattern with a prominent subsurface rate maximum (Fig. 2e-g). The rates were consistently low to undetectable in the upper mixed layer where nutrients were depleted at all stations, and increased rapidly to the depth of maximum rate (Fig. 2). Ammonia and urea oxidation rates peaked at shallower depths (90-170 m) compared to the depth of the highest nitrite oxidation rate (130-200 m, Table S2). The depth of the rate maximum was correlated with biological productivity (inferred from the depth and the magnitude of florescence in the DCM), which determines the light attenuation and substrate supply for ammonia and nitrite oxidizers in the ocean (Tang et al., 2023). Ammonia oxidation rate (ranging from below the

317 detection limit to 40.48 nmol N L^{-1} d^{-1}, median 1.67 nmol N L^{-1} d^{-1}) was, in general, higher than
318 that of urea oxidation (from below the detection limit to 18.95 nmol N L^{-1} d^{-1}, median 1.53 nmol
319 N L^{-1} d^{-1}) in the epipelagic layer; however, the opposite was observed in the mesopelagic layer
320 (i.e., ammonia oxidation ranged from below the detection limit to 4.09 nmol N L^{-1} d^{-1}, median 0.12
321 nmol N L^{-1} d^{-1} ; and urea oxidation ranged from below the detection limit to 2.79 nmol N L^{-1} d^{-1},
322 median 0.32 nmol N L^{-1} d^{-1}) due to the slower attenuation of urea oxidation rate relative to
323 ammonia oxidation in the ocean's interior (Fig. 2e, f, inserted panels), where NH_4^+ concentration
324 further decreased. However, the difference between ammonia oxidation and urea oxidation was
325 not statistically significant owing to the large variation of both rates along the water column
326 (p>0.05). Above the depth of maximum ammonia oxidation rate, nitrite oxidation rate (from below
327 the detection limit to 2.95 nmol N L^{-1} d^{-1}) was lower than that of ammonia oxidation at the
328 corresponding depths. The relationship was reversed at greater depths (i.e., from below the
329 detection limit to 6.35 nmol N L^{-1} d^{-1}, and from below the detection limit to 11.26 nmol N L^{-1} d^{-1},
330 for ammonia and nitrite oxidation, respectively) (Fig. 2g).

331 The depth-integrated (0-1000 m) urea oxidation rate was 0.5 to 2.5 times higher than the
332 integrated ammonia oxidation rate (median: 0.77), suggesting a substantial contribution of urea
333 oxidation to NO_2^- production in the oligotrophic ocean (Table 1). The integrated ammonia
334 oxidation rate was consistently lower than nitrite oxidation rate at all stations, due to the low
335 ammonia oxidation rates in the mesopelagic zone.

336 **3.3 L-Glutamic acid-derived nitrogen oxidation rate**

337 ^{15}N-Urea (100 nmol N L^{-1}) and ^{15}N-Glu (100 nmol N L^{-1}) derived nitrogen oxidation rates
338 with or without the addition of unlabeled NH_4^+ (2000 nmol N L^{-1}) were measured at four stations
339 in the NWP. Without added NH_4^+, ^{15}N-NO_2^- production rate from both ^{15}N-Urea and ^{15}N-Glu
340 followed similar spatial patterns across stations and depths. The rate was generally higher from
341 ^{15}N-Glu (0.01-18.3, median 4.2 nmol N L^{-1} d^{-1}) than from ^{15}N-Urea (0.02-13.4, median 2.2 nmol
342 N L^{-1} d^{-1}), even though the two groups of rates were not statistically significant (p>0.05) (Fig. 3).
343 The addition of unlabeled NH_4^+ decreased the ^{15}N-NO_2^- production rate in both ^{15}N-Urea and ^{15}N-
344 Glu incubations. The effect was greater for the ^{15}N-Glu treatment; 9 of 15 depths showed a
345 significant difference in ^{15}N-NO_2^- production rate with and without unlabeled NH_4^+ amendment
346 for ^{15}N-Urea (Fig. 3a), compared to 14 of 15 depths for ^{15}N-Glu (Fig. 3b). The decrease in ^{15}N-

NO_2^- production rate with NH_4^+ addition for ^{15}N-Urea (6-86%, median 51%) was significantly less than the decrease for ^{15}N-Glu (15-99%, median 92%) (p<0.001).

3.4 Kinetics of ammonia, urea and nitrite oxidation

The dependence of ammonia, urea, and nitrite oxidation rates on substrate concentration (*in-situ* concentration plus tracer) was investigated by adding different amounts of tracers at selected stations in the NWP and the wNPSG (Fig. 4). Notably, not all the depths showed the typical M-M type response to substrate enrichment, i.e., for ammonia oxidation, only 4 of total 15 depths in the NWP cruise, and 6 of 12 depths in the wNPSG cruise could be fitted using the M-M equation. Similarly, 5 of 12, and 6 of 12 depths demonstrated M-M type kinetic response for urea oxidation and nitrite oxidation, respectively, in the wNPSG cruise. Lack of kinetic response was often due to undetectable rates at all substrate levels in surface samples, but also occurred at other depths in the lower euphotic and mesopelagic zone.

For the depths that showed M-M type responses, the V_{max} of ammonia oxidation varied over three orders of magnitude (ranging from <0.1 nmol L^{-1} d^{-1} in the surface layer of station K11 in the SCS to > 100 nmol L^{-1} d^{-1} at the base of the euphotic zone in the more productive B1 station in the NWP (Fig. 4a, b). The highest V_{max} values occurred in the vicinity of the PNM layer where the maximum *in-situ* ammonia oxidation rates occurred (Wan et al., 2021). V_{max} also varied spatially, and was higher in the more productive NWP than the oligotrophic wNPSG. Likewise, the K_s values for NH_4^+ ranged from 24 nmol L^{-1} to 390 nmol L^{-1}, and were higher in the NWP stations (67-390 nmol L^{-1}, median 122 nmol L^{-1}) than the wNPSG stations (24-219 nmol L^{-1}, median 42 nmol L^{-1}). The co-varying V_{max} and K_s values observed here reveal the higher potential ammonia oxidation capacity and higher requirement of substrate to reach V_{max} of the ammonia-oxidizing community in the more productive marine environment, suggesting that both V_{max} and K_s of AOA natural populations are largely regulated by primary productivity as labile organic decomposition is the major source of NH_4^+ in the ocean (e.g., Gruber, 2008; Santoro et al., 2019; Ward and Zafiriou, 1988).

The kinetics of urea oxidation had a pattern similar to that of ammonia oxidation, with the highest V_{max} located in the vicinity of the PNM layer at the wNPSG stations (i.e., 100-140m, Table S2). However, for those stations and depths where the kinetics of both ammonia oxidation and

urea oxidation were determined, the measured V_{max} for urea oxidation (1-19 nmol N L^{-1} d^{-1}, median 3 nmol N L^{-1} d^{-1}) was lower than for ammonia oxidation (p<0.01), and the K_s value (97-263 nmol N L^{-1}, median 154 nmol N L^{-1}) was higher than for ammonia oxidation (p<0.01) (Fig. 4c).

Unlike ammonia and urea oxidation, the highest V_{max} of nitrite oxidation was not consistently located at the PNM depth at the wNPSG stations (Fig. 3; Table S2), and the depth with the highest *in-situ* nitrite oxidation rate was not captured for kinetic analysis. Thus, a relationship between the magnitude of V_{max} and the depth distribution of nitrite oxidation cannot be discerned. The K_s value of nitrite oxidation ranged from 61-225 nmol L^{-1} (median 90 nmol L^{-1}), which was higher than the K_s value of ammonia oxidation, but was lower than the K_s value of urea oxidation at the corresponding depths (Fig. 4d).

3.5 Distribution of urea oxidation and ammonia oxidation in the ocean

Our data compilation shows that in the heavily human-perturbed estuarine and coastal waters, including the Gulf of Mexico, the Chesapeake Bay, the Coast of Georgia, the East China Sea and the Jiulong River Estuary, urea and NH_4^+ concentrations were significantly correlated (R^2 = 0.6; p<0.001), although both concentrations varied widely; urea concentration ranged from 0.03 to 5.35 μmol N L^{-1} (median 0.53 μmol N L^{-1}), and NH_4^+ ranged from 0.03 to 59 μmol L^{-1} (median 1 μmol L^{-1}) (Fig. 5a; Fig. 6a). The correlation is probably due to the fact that both urea and NH_4^+ in these coastal waters are largely sourced from human activities such as fertilization and wastewater discharge (Sipler and Bronk, 2015). By comparison, urea and NH_4^+ concentrations were much lower in the wNPSG, the NWP, and the Arctic and Antarctic Oceans, and no significant correlation was found between them in the epipelagic or mesopelagic zone (Fig. 5a). In contrast to the coastal water, urea concentration appears to be higher than NH_4^+ concentration in these open ocean systems; the median urea concentrations in the epipelagic and mesopelagic zone were 92 and 63 nmol N L^{-1}, respectively, while the corresponding median NH_4^+ concentrations are 31 and 9 nmol N L^{-1} (Fig. 6a). Accordingly, the urea to NH_4^+ ratio shows a stepwise increase, with admittedly large ranges, from the coastal water (median 0.3) to the epipelagic zone (median 3.1), and to the mesopelagic ocean (median 6.6) (Fig. 6c).

Both the urea and ammonia oxidation rates vary over four orders of magnitude in the coastal water. Urea oxidation rate ranges from 0.1 to 296 (median 7) nmol N L^{-1} d^{-1}, and ammonia

oxidation rate varies from 0.4 to 6541 (median 314) nmol N L^{-1} d^{-1} (Fig. 6b). For the open ocean system, urea oxidation and ammonia oxidation rates are significantly correlated in the epipelagic zone, with the median values of 2 and 7 nmol N L^{-1} d^{-1}, respectively (Fig. 6b). The two rates further decline to 0.5 and 0.3 nmol N L^{-1} d^{-1}, respectively, in the mesopelagic zone. Similar to the concentration ratio distribution, the urea oxidation to ammonia oxidation rate ratio also shows a stepwise increase from the coastal water (0.0004 to 5.4, median 0.03) to the epipelagic zone (0.008 to 2.9, median 0.4), and to the mesopelagic ocean (0.004 to 7.0, median 1.2). The rate ratio was significantly higher in the mesopelagic zone than the coastal and epipelagic zone (p<0.01) (Fig. 6d).

4. Discussion

4.1 Distinct fate of urea- and glutamic acid-derived nitrogen implies direct oxidation of urea to nitrite

Whether the observed urea oxidation is performed by ammonia oxidizers or through the decomposition of urea by other microbes followed by ammonia oxidation, or both, is unclear, as different lines of evidence lead to inconsistent conclusions. By comparing the urea oxidation rate obtained from ^{15}N-Urea labeling with or without added $^{14}NH_4^+$, direct urea oxidation is reported to account for over 50% of the measured bulk urea oxidation rate in the Gulf of Mexico (Kitzinger et al., 2019). In the Arctic Ocean and the Central Equatorial Pacific, the significant correlation between archaeal *amoA* and *ureC* gene abundance also points to the potential direct urea oxidation by marine AOA (Alonso-Sáez et al., 2012; Santoro et al., 2017). However, that conclusion was not supported by transcriptional data showing no transcription of *ureC* in the Northeast Pacific (Smith et al., 2016). In our study, a significant fraction of ^{15}N-Urea derived nitrogen was oxidized to $^{15}N\text{-}NO_2^-$ even in the presence of added $^{14}NH_4^+$, which reduced the measured $^{15}N\text{-}NO_2^-$ production rate by 6-86% (median 51%) (Fig. 3a). The ^{15}N-urea to $^{14}NH_4^+$ concentration ratio was less than 0.05 in the ^{15}N-urea plus $^{14}NH_4^+$ amendment experiment. By comparison, the ratio of ^{15}N-urea to $^{14}NH_4^+$ in the *in-situ* water was >1 without $^{14}NH_4^+$ carrier amendment. Assuming the measured urea oxidation rate was sourced from urea decomposition by other microbes followed by ammonia oxidation (i.e., all by indirect urea oxidation pathway), we would expect to observe a 20-fold difference (95% reduction) of $^{15}N\text{-}NO_2^-$ production rate in the treatment with ^{15}N-urea plus $^{14}NH_4^+$ amendment compared to ^{15}N-urea only treatment. In contrast, our measured results showed

435 a median of only 2-fold difference (51% reduction) between the two treatments. The results thus
436 suggest that a large fraction of the measured $^{15}N\text{-}NO_2^-$ production rate in the ^{15}N-urea plus $^{14}NH_4^+$
437 treatment was due to direct urea oxidation. Alternatively, a direct linkage between urea degradation
438 and ammonia oxidation in a microbial consortium with the NH_4^+ released by urea decomposition
439 directly accessed by ammonia oxidizers without exchange with the ambient water, such as the
440 reciprocal feeding of ammonia oxidizers and ureolytic NOB (Koch et al., 2012) or cyanate-
441 degrading NOB (Palatinszky et al., 2015), may also lead to a lesser decrease than the predicted
442 value. However, more experimental evidence is needed to test this hypothesis.

443 The ^{15}N-Glu derived NO_2^- production rate was higher than the rate in the ^{15}N-urea treatment
444 at the same tracer concentration (i.e., median: 4.2 and 2.2 nmol N L^{-1} d^{-1}, respectively) and unlike
445 ^{15}N-urea, decreased dramatically (median 92%) upon addition of $^{14}NH_4^+$ (Fig. 3b). This is a nearly
446 12.5-fold difference due to $^{14}NH_4^+$ addition between urea and glutamate as a source of NO_2^-. This
447 result was more consistent with the 95% decrease predicted from the coupled heterotrophic
448 decomposition-ammonia oxidation pathway. Although the *in-situ* glutamate concentration was not
449 measured in our study, previous measurements show an extremely low free glutamate
450 concentration (< 1 nmol L^{-1}) in the open ocean (Pèrez et al., 2003; Suttle et al., 1991), indicating
451 a tight linkage between glutamate decomposition and ammonia oxidation or assimilation. The
452 NH_4^+ sourced from glutamate decomposition thus apparently needs to be released to the ambient
453 water before being accessed by the ammonia oxidizers, which was also observed in the South
454 Atlantic Bight (Damashek et al., 2019). Combing the results of the distinctive response of ^{15}N-
455 urea and ^{15}N-Glu derived nitrogen oxidation to $^{14}NH_4^+$ addition, we suggest that the observed
456 $^{15}NO_2^-$ production in the ^{15}N-urea plus $^{14}NH_4^+$ addition treatment was largely sourced from direct
457 urea oxidation. By comparison, the majority of ^{15}N-Glu supported $^{15}N\text{-}NO_2^-$ production was via
458 coupled glutamate decomposition-ammonia oxidation. These results revealed a distinct fate and
459 role for different forms of labile DON in marine nitrification.

460 **4.2 Urea oxidation helps to balance the two steps of nitrification in the oligotrophic ocean**

461 A recent compilation of ammonia oxidation and nitrite oxidation rate measurements in the
462 global ocean shows decoupling of the two steps in nitrification, with the nitrite oxidation rate
463 maxima generally located below the depth of ammonia oxidation rate maxima, and nitrite
464 oxidation frequently exceeding ammonia oxidation rate below the euphotic zone in the open ocean

systems (Tang et al., 2023). Thus, not only are the rates vertically decoupled, but excess nitrite oxidation may indicate a missing of NO_2^- source in the dark ocean. Recent studies find urea-derived nitrogen contributes ~20-30% of NO_2^- production compared to ammonia oxidation, playing an additional role in NO_2^- production and PNM formation in the sunlit ocean (Laperriere et al., 2021; Wan et al., 2021). Our new data compilation revealed that the oxidation of urea-derived nitrogen accounts for 27% (median value) of total NO_2^- production from urea and ammonia in the epipelagic zone, and the contribution increased to 55% in the mesopelagic zone, suggesting an increasing role of urea oxidation in NO_2^- production in the dark ocean, which might influence the balance of the two steps of nitrification.

To further quantify the role of urea in regulating the balance of NO_2^- production and consumption during marine nitrification, we compared the rates of NO_2^- oxidation and total NO_2^- production from ammonia and urea oxidation in our dataset collected in 2021 from the SCS and the wNPSG. Given the different contribution of urea oxidation to NO_2^- production and the distinct AOA communities in the epipelagic and mesopelagic ocean, we separately compared NO_2^- production and consumption in these two layers (Fig. 7a, b). The results showed that the nitrite oxidation rate was lower than the total NO_2^- production rate by ammonia oxidation plus urea oxidation (the ratio was 0.70±0.10) in the epipelagic zone, suggesting excess NO_2^- production by ammonia oxidizers (Fig. 7a). The ratio increased to 0.91±0.15 in the mesopelagic zone, indicating nearly balanced NO_2^- production and consumption (Fig. 7b). Thus, urea oxidation plays an essential role in maintaining the balance of the two steps of nitrification in the oligotrophic ocean (Fig. 7c). Although the potential utilization of other labile DON species, such as cyanate (Kitzinger et al., 2019; Palatinszky et al., 2015) and polyamine (Damashek et al., 2019), by marine ammonia oxidizers has also been reported in lab and field studies, the contribution of these compounds to NO_2^- production is probably limited in the oligotrophic ocean for the following reasons. Firstly, cyanate and polyamine undergo rapid abiotic or biotic decomposition by heterotrophs in the ocean, and therefore are usually present at trace levels (an order of magnitude lower than urea) (Liu et al., 2022; Lu et al., 2014; Kitzinger et al., 2019; Widner et al., 2016). Secondly, the absence of known metabolic genes or pathways for cyanate and polyamine hydrolysis in marine ammonia oxidizers suggests that the metabolism of these organic N substrates may occur through alternative and potentially less efficient indirect processes (Damashek et al., 2019; Santoro et al., 2019). Thirdly, compared to cyanate and polyamine, urea is chemically more stable, supporting its higher standing

stock (Sipler and Bronk, 2015), and many marine ammonia oxidizers possess urea transport and hydrolysis genes (Bayer et al., 2016; Qin et al., 2024). These lines of evidence suggest that urea oxidation might be primarily responsible for DON-derived NO_2^- production by marine ammonia oxidizers in the oligotrophic ocean.

4.3 Kinetic traits determine marine NH_4^+, urea and NO_2^- distribution

Substrate affinity is considered a key trait in determining the capability of microbes to access and compete for substrate when it becomes limiting. NH_4^+, urea, and NO_2^- are all present at nanomolar concentrations in most open ocean systems and marine nitrifiers possess high affinity towards the trace substrates. Less than half of the depths (10 of the total 27 depths for ammonia oxidation, 5 of 12 depths for urea oxidation, and 6 of 12 depths for nitrite oxidation) investigated here demonstrated M-M type response to substrate enrichment (Fig. 4). The samples did not show M-M type response were grouped into three types: i) The rate was below the detection limit at the low substrate end or the rate was too low to be detected at all tested substrate concentrations. These samples were mainly located at the surface layer (5 m) and the deeper mesopelagic zone (> 800 m). Marine ammonia and nitrite oxidizers are known to be sensitive to light, and are outcompeted by phytoplankton at the surface of the oligotrophic ocean (Santoro et al., 2019; Wan et al., 2021). Thus, the lack of detectable rate is likely due to the absence of nitrifiers or lack of nitrification activity in the surface water (Fig. 2) (Santoro et al., 2019; Tang et al., 2023). For the deep water, both the abundance and activity of nitrifiers are restricted by substrate supply; this is particularly the case in the oligotrophic ocean where the organic flux is very low. Although the geochemical data, e.g., the accumulation of NO_3^- and consumption of dissolved oxygen in the deep water, provide evidence of the occurrence of nitrification in the ocean's interior, the activity of nitrifiers (and their low abundance) prohibits the detection of the oxidation rates in short-term incubations. ii) The rate was detectable but showed no response to substrate enrichment, typically observed at the depths with relatively high substrate concentration, such as ammonia oxidation at the coastal C3 station and the mid-latitude B1 station, as well as nitrite oxidation at the base of the euphotic zone at K11 and K8a stations. The lack of rate enhancement by adding substrate could result from either substrate saturation or factors other than substrate concentrations, such as the trace metals iron and cooper, in limiting the rate (Horak et al., 2013; Shiozaki et al., 2016; Ward, 2008). In our study, substrate saturation is probably the main cause of the lack of M-M type response in the

coastal and more productive mid-latitude stations, while for the remote wNPSG stations, iron or copper limitation is more likely responsible for the absence of kinetic response, as our study area region is characterized by low iron and copper concentrations (König et al., 2021; Richon and Tagliabue, 2019). iii) We found a decrease in ammonia oxidation rate with ^{15}N-NH_4^+ enrichment at some depths at stations K6, A8 and B1 in our study. This unexpected apparent inhibition of ammonia oxidation by substrate was unlikely caused by the ammonia toxicity as the highest NH_4^+ concentration in our experiment was ~1 μmol L^{-1}, a level that is much lower than all known NH_4^+ inhibition concentrations for nitrifiers (Liu et al., 2021), even though a potential inhibition effect under such low NH_4^+ concentration cannot be fully excluded. A recent study reported inhibition of urea oxidation rate by urea enrichment in the Arctic Ocean, which was explained by stimulation of NH_4^+ generation by the high urea amendment, and inhibition of urea utilization by the resulting elevated NH_4^+ concentration (Shiozaki et al., 2021). However, such a result is not observed in our urea oxidation kinetic experiments, and cannot explain the apparent inhibition in our NH_4^+ enrichment experiment. A study conducted in the Southern Ocean finds a similar inhibition of ammonia oxidation rate by high $^{15}NH_4^+$ amendment (~1 μmol L^{-1}) in waters with relatively high *in-situ* NH_4^+, and is interpreted as a substrate saturation condition, but the potential cause for the apparent inhibition is not discussed (Mdutyana et al., 2022b). Currently, we are unable to resolve the decrease of ammonia oxidation rate at NH_4^+ enrichment of ~1 μmol L^{-1}; future studies are warranted to examine the ubiquity and underlying reason for such an intriguing response.

For depths that exhibited typical M-M type kinetic response, the K_s of ammonia oxidation and nitrite oxidation varied between 24-390 nmol L^{-1}, and 61-225 nmol L^{-1}, falling in the range of reported K_s in the open ocean systems (e.g., Liu et al., 2023; Mdutyana et al., 2022; Wan et al., 2018). For urea oxidation, the K_s varied in the range 97-263 nmol N L^{-1}, which was higher than the K_s for NH_4^+ at the corresponding depths, suggesting a higher affinity towards NH_4^+ in marine AOA. This result is consistent with a recent pure culture-based investigation showing that the ureolytic marine AOA species possess higher affinity towards NH_4^+ than urea (Qin et al., 2024). We further added our results to a recently compiled dataset (Liu et al., 2023) to investigate the spatial distribution of the K_s in the ocean. The results exhibited a power law profile of K_s for ammonia oxidation and nitrite oxidation as a function of water depth, although some data points measured in the mesopelagic zone of the SCS and the NWP stations were higher than the fitted values (Fig. 8a, c). This increase in affinity for NH_4^+ and NO_2^- at greater depths suggests adaptation

to the more limiting substrate levels at depth for AOA and NOB. By comparison, no significant vertical pattern was found for the K_s of urea oxidation, despite the fact that the highest K_s was observed in the upper euphotic zone (40 m) and the lowest K_s was observed in the mesopelagic zone (270 m) (Fig. 8b). This lack of significant vertical trend might result from insufficient observations (n=9), particularly the lack of observation in the mesopelagic zone (i.e., only one data point).

The statistics of K_s showed that the affinity for NH_4^+ was highest (lowest K_s value) compared to urea and NO_2^- at corresponding depths (Fig. 8), demonstrating the higher capability of marine nitrifiers in scavenging NH_4^+ relative to urea and NO_2^-. For urea and nitrite oxidation, the K_s value was comparable in the euphotic zone, with the affinities for both substrates being relatively low. The K_s for NO_2^- decreased towards the greater depth to the minimum value of 27 nmol L^{-1}, while the lowest K_s value for urea remained at ~100 nmol N L^{-1}. These kinetic traits help to explain the observed NH_4^+, urea and NO_2^- distributions in the ocean, i.e., due to the limited supply of labile organic matter to the ocean's interior. The ammonia- and nitrite-oxidizing microbes are therefore limited by the substrate supply, and maintain the substrate concentrations at their lowest accessible level in the dark ocean. In our study, high NH_4^+ concentrations were detected sporadically in the euphotic zone, but at consistently low levels, i.e., < 10 nmol L^{-1} in the mesopelagic zone. NO_2^- concentration was also low except for the PNM at the base of the euphotic zone. By contrast, urea was present at higher concentration than NH_4^+ and NO_2^- throughout the water column except in the NH_4^+ maximum and PNM layers. The kinetic results showed that in the euphotic zone, where relatively high NH_4^+ and NO_2^- concentrations were observed, the K_s values were also elevated although the values varied across different regions. Nevertheless, the K_s values in the euphotic zone were statistically higher compared to the mesopelagic zone (p<0.001), suggesting the accumulation of $NH_4^+$and NO_2^- was at least partly due to the low affinity of nitrifiers in accessing the substrates. Below the euphotic zone, we observed consistently low NH_4^+ and NO_2^- concentrations in the mesopelagic zone compared to the euphotic zone. This pattern was consistent with the K_s of NH_4^+ and NO_2^-, which decreased with water depth, leading to effective scavenging of NH_4^+ and NO_2^- by AOA and NOB in the dark ocean. Compared to NH_4^+ and NO_2^- concentration, urea concentration did not decrease sharply and was higher in the dark ocean, accompanied with the higher K_s of urea oxidation. These results suggest the affinities of AOA and NOB in accessing

their substrates might be important in controlling the distribution of NH_4^+, urea, and NO_2^- in the open ocean.

4.4 Geographic distribution of urea oxidation and ammonia oxidation in the ocean

Since the first report of urea oxidation by marine AOA in the Arctic Ocean (Alonso-Sáez et al., 2012), urea oxidation has been investigated in several marine systems extending from coastal to open ocean, providing direct evidence for the contribution of urea in supporting energy metabolism for marine ammonia oxidizers. However, the relative magnitudes of urea oxidation and ammonia oxidation vary greatly among different regions, i.e., the ratio of urea oxidation to ammonia oxidation ranges from less than 1% in the hyper-eutrophied Jiulong Estuary (J. M. Tang et al., 2022) to over 200% in the Arctic and Antarctic oceans (Shiozaki et al., 2021; Tolar et al., 2017). The cause for such high variability across different systems remains unexplained. A substantial subset of ammonia oxidizers possess the genetic capability to utilize both ammonia and urea, and their substrate preference and regulation of urea and NH_4^+ utilization vary among major lineages (Qin et al., 2024). Thus, urea utilization may represent a key mechanism for niche partitioning and adaptation of ammonia oxidizers to different environmental settings.

The results of our data compilation suggest a geographic distribution pattern of urea oxidation and ammonia oxidation in the ocean (Fig.5, 6). Both rates decrease from the coastal to the open ocean and urea oxidation becomes relatively more important compared to ammonia oxidation along the same gradient. The increasing ratio of urea oxidation to ammonia oxidation rate parallels the increase in the urea: NH_4^+ concentration ratio, indicating regulation of NH_4^+ and urea utilization strategy in marine ammonia oxidizers by the relative substrate concentration. This result is also congruent with the spatial pattern of archaeal *ureC* and *amoA* gene distribution showing an increasing trend of *ureC*: *amoA* ratio from the coastal water to open ocean. For instance, *ureC*: *amoA* ratio is 16-23% in the Coast of Georgia (Tolar et al., 2017) and 10-15% in the Gulf of Mexico (Kitzinger et al., 2019). By comparison, the *ureC*: *amoA* ratio increases to 22-55% in the Equatorial Pacific (Santoro et al., 2017), and exceeds 1 at the PNM depth at station ALOHA (Qin et al., 2020) and in the deep water of the Arctic Ocean (Alonso-Sáez et al., 2012) and the Antarctic Ocean (Tolar et al., 2017).

These variations in urea and ammonia oxidation rates translate into variable contributions to NO_2^- production in the open ocean. The high urea oxidation to ammonia oxidation rate ratio in the mesopelagic ocean reveals an important role for urea oxidation in NO_2^- production in the ocean's interior that has not been appreciated. Depth-integrated (0-1000m) urea oxidation and ammonia oxidation rates were comparable in the SCS and the wNPSG (Table 1). If the same scale applies to the global ocean, NO_2^- production rates by ammonia oxidizers in the ocean might currently be underestimated substantially if NH_4^+ is considered the only substrate for marine AOA. We note, however, future efforts should be devoted to quantifying the contribution of direct versus indirect urea oxidation, and more measurements of urea and ammonia oxidation across the ocean are needed to better assess the NO_2^- production budget in the global ocean. Moreover, given that ammonia oxidizers play a key role in marine dark carbon fixation (Herndl et al., 2013; Zhang et al., 2020) and nitrous oxide production (Ji et al., 2018; Wan et al., 2023), our results also indicate a potential role of urea oxidation in the marine carbon cycle and greenhouse gas production that should be investigated in the future.

5. Conclusions

Our measurements of nitrogen nutrient distribution, ammonia, urea, and nitrite oxidation rates and their dependence on substrate concentration across a wide range of the SCS and the wNPSG provided several new insights into marine nitrification. In particular, we demonstrated that urea oxidation is an important process for balancing the two steps of nitrification, contributing even more NO_2^- than ammonia oxidation in the mesopelagic zone of the oligotrophic ocean, indicating the need to revisit the nitrification flux, and the associated dark carbon fixation, nitrous oxide production, and dissolved oxygen consumption in the ocean's interior.

We observed distinct patterns of kinetic responses to substrate enrichment. The K_s of ammonia oxidation and nitrite oxidation fall in the range of reported values and had a depth distribution that could be described by a power law, suggesting increased affinity in accessing the decreasing substrate concentrations in the energy-starved dark ocean. No clear vertical pattern was detectable for the K_s values of urea oxidation, which were higher than the K_s of ammonia oxidation at corresponding depths. The underlying reason for the higher K_s of urea oxidation may be related to the different mechanism in accessing NH_4^+ and urea, and/ or the impact of indirect urea oxidation that is associated with another process carried out by different organisms and governed

by their own kinetic parameters. Nevertheless, the result supports the recent finding of the preferential use of NH_4^+ by marine AOA (Qin et al., 2024), and explains the higher standing stock of urea than NH_4^+ in the oligotrophic ocean. We also found that a considerable fraction of samples showed no response to substrate enrichment due to absence of a viable nitrifying assemblage in surface waters, the *in-situ* substrate concentration being saturated, or rate limitation by some factor other than substrate. Finally, a contrasting response of ^{15}N-Urea and ^{15}N-Glu oxidation to $^{14}NH_4^+$ amendment indicated that a large fraction of urea was directly oxidized by marine AOA. In contrast, nearly all glutamate-derived ammonia oxidation was driven by coupled heterotrophic decomposition and ammonia oxidation, suggesting distinctive fates of different DON compounds in sustaining NO_2^- production. These findings provide new information to improve models for understanding and predicting nitrogen biogeochemistry in the ocean.

Figures

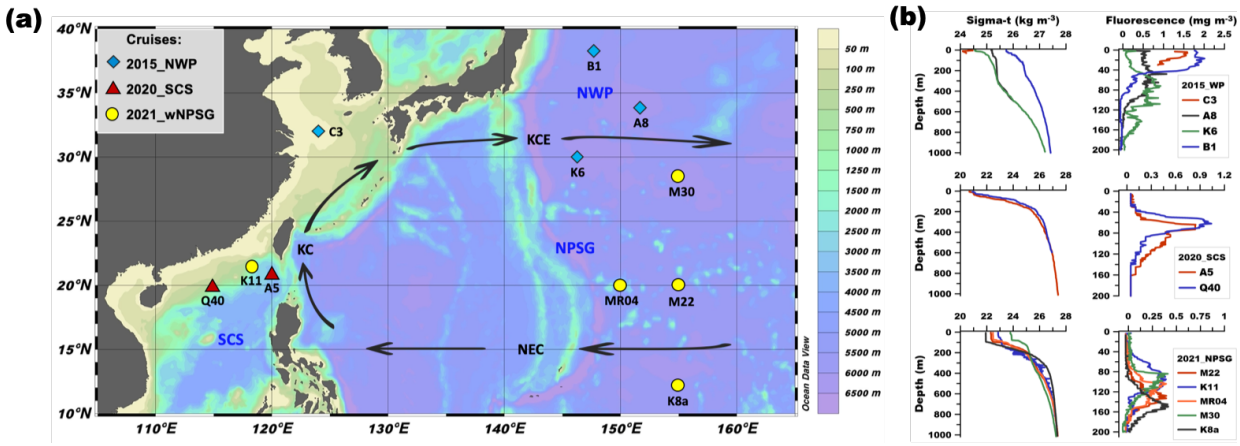

Fig. 1 Study area and physical properties of the sampling stations. (a) Research area and sampling stations. Diamonds, triangles and dots show stations during the 2015 NWP, 2020 SCS, and 2021 wNPSG cruises, respectively. The black arrows denote the main surface currents of the NPSG. NEC, KC and KCE are abbreviations of the North Equatorial Current, Kuroshio Current, and Kuroshio Current Extension, respectively. (b) Potential density anomaly and fluorescence profiles of the sampling stations during each cruise.

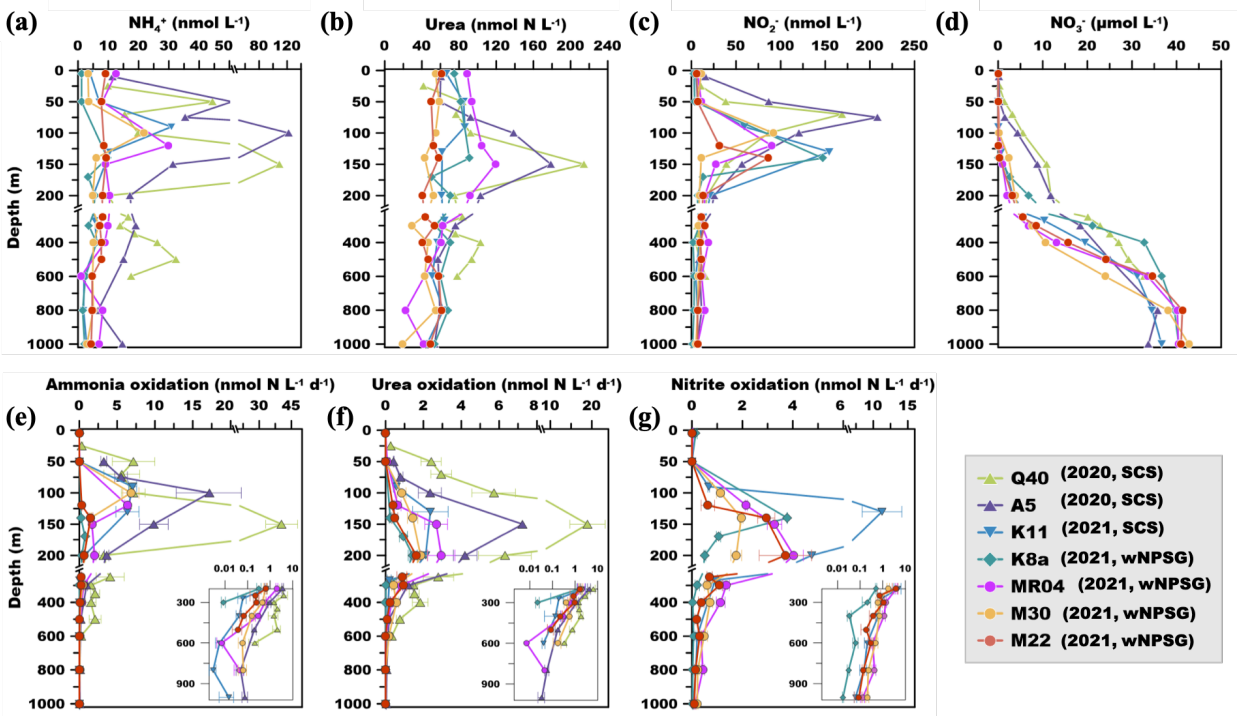

Fig. 2 Nitrogen nutrient distribution and nitrification rate profiles. (a-d) Depth profiles of NH_4^+, Urea, NO_2^-, and NO_3^- in the SCS and the wNPSG stations, respectively. (e-g) *In-situ* rates of ammonia oxidation, urea oxidation and nitrite oxidation, respectively. The error bars denote one standard deviation of triplicate rate measurements; in some cases, the error bars are smaller than the symbols. The insert panels depict the rate in the mesopelagic zone; note the rates in the insert panels are shown in log scale.

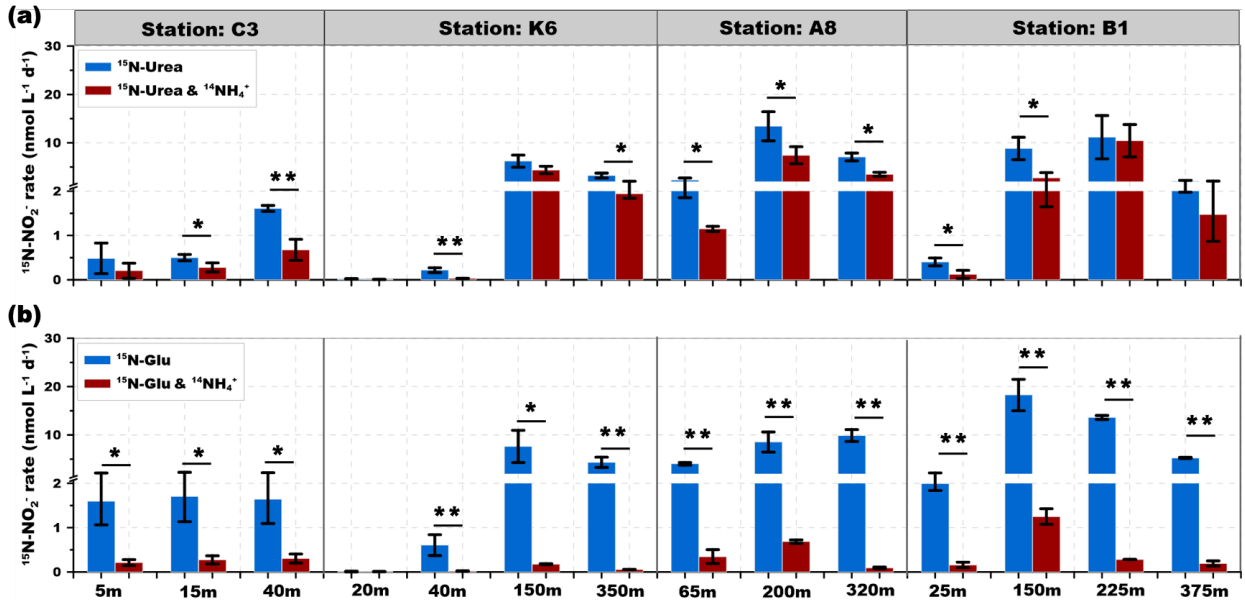

Fig. 3 Comparison of urea and glutamic acid derived nitrogen oxidation. (a) ^{15}N-NO_2^- production rate in the ^{15}N-Urea labeling experiment. (b) ^{15}N-NO_2^- production rate in the ^{15}N-Glu labeling experiment. The blue bars and red bars depict the production rates without or with unlabeled NH_4^+ amendment, respectively. The error bars denote one standard deviation of triplicate rate measurements. (*) and (**) show the significance at 0.05 and 0.01 levels (*t* test), respectively.

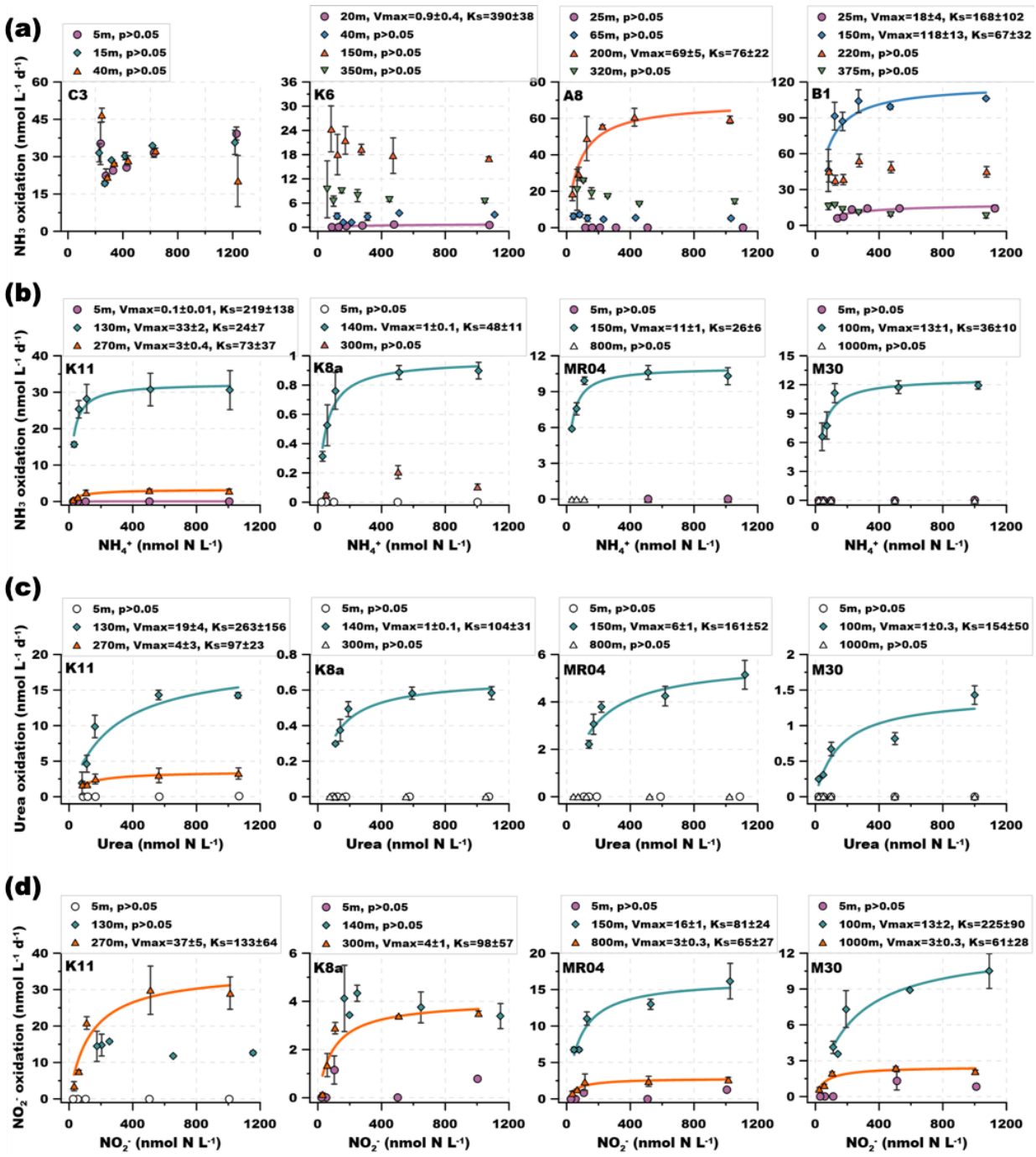

Fig. 4 Kinetic behavior of ammonia, urea and nitrite oxidation. (a-b) The dependence of ammonia oxidation rate on total NH_4^+ concentration (*in-situ* plus tracer concentration) in selected NWP (C3, K6, K8, B1), SCS (K11) and wNPSG (K8a, MR04, M30) stations, respectively. (c-d) The dependence of urea and nitrite oxidation rate on total urea and NO_2^- concentration, respectively, in the SCS and wNPSG stations. The filled shapes indicate detectable rates, and the

open shapes indicate rates below the detection limits. The error bars denote one standard deviation of triplicate rate measurements; in some cases, the error bars are smaller than the symbols. The solid lines represent the fitted M-M curves for depths that show significant relationship (p<0.05) between substrate concentrations and rates.

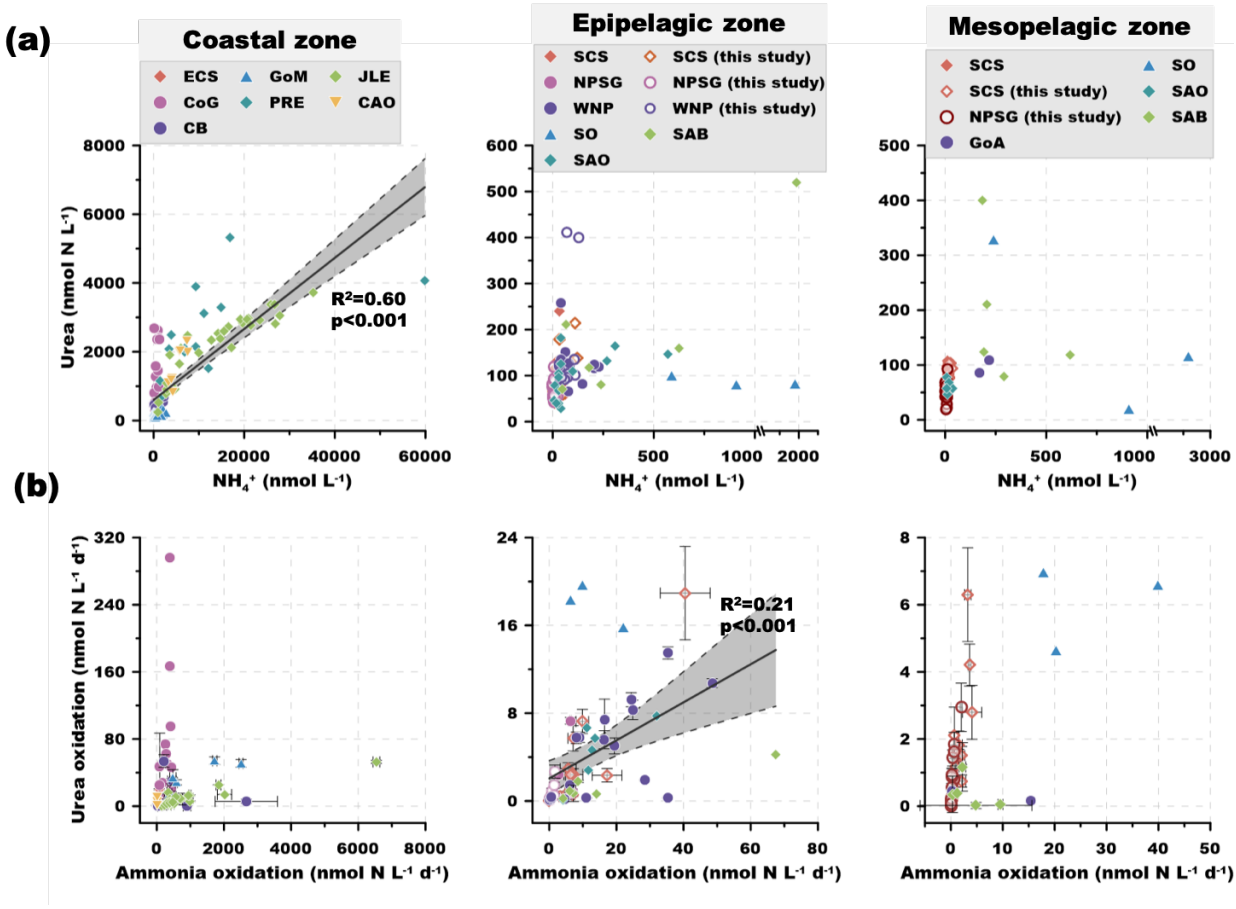

Fig. 5 Compilation of urea and NH_4^+ concentrations and the oxidation rates measured in the global ocean. (a) Urea and NH_4^+ concentrations; (b) Urea and ammonia oxidation rates. The dataset is divided into three groups: the coastal zone, the epipelagic zone, and the mesopelagic zone. Data source for the coastal zone includes the East China Sea (ECS) (Xu et al., 2019), the Gulf of Mexico (GoM) (Kitzinger et al., 2019), the Jiulong Estuary (JLE) (J. M. Tang et al., 2022), the coast of Georgia (CoG) (Damashek et al., 2019; Tolar et al., 2017), the Pearl River Estuary (PRE) (Chen et al., 2015), coast of the Arctic Ocean (CAO) (Shiozaki et al., 2021), and the Chesapeake Bay (CB) (W. Tang et al., 2022). Date source for the open ocean includes the South China Sea (SCS) (Chen et al., 2015), the North Pacific Subtropical Gyre (NPSG) and the

699 Northwestern Pacific (NWP) (Wan et al., 2021; Xu et al., 2019), the Southern Ocean (SO); the
700 South Atlantic Bight (SAB), the slope of Arctic Ocean (SAO) and the Gulf of Alaska (GoA)
701 (Damashek et al., 2019; Tolar et al., 2017; Shiozaki et al., 2021), and rates measured in the SCS,
702 NWP, and wNPSG from this study.

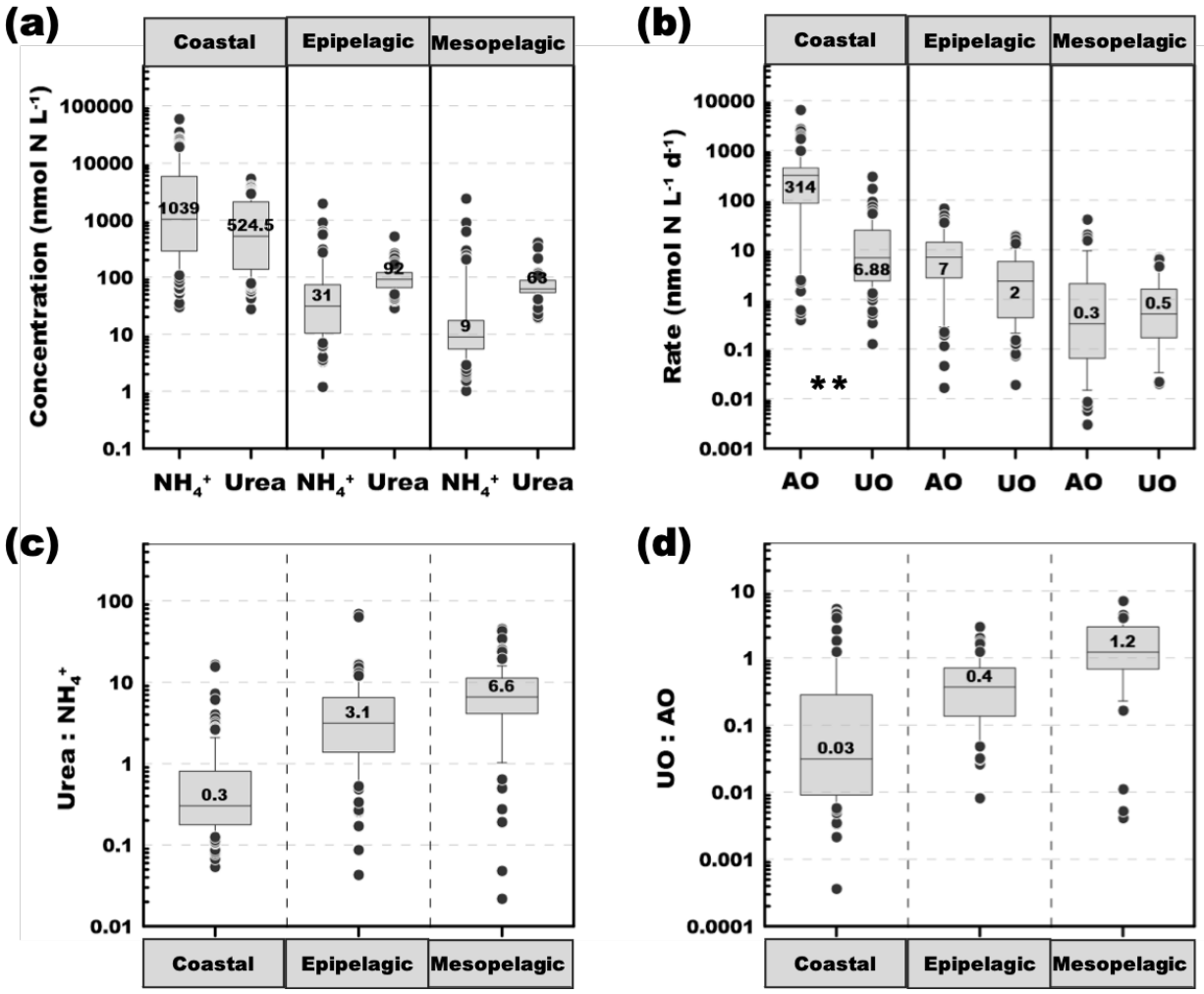

703

704 **Fig. 6 Box plots of urea and NH_4^+ concentrations and oxidation rates in the ocean.** The data
705 sources are shown in Fig. 6. (a) NH_4^+ and urea concentration; (b) Ammonia and urea oxidation
706 rate; (c) Statistics of NH_4^+ and urea concentration; (d) Statistics of ammonia and urea oxidation
707 rate. AO and UO are ammonia oxidation and urea oxidation rates. The numbers in the box plots
708 show the median value, whiskers and boxes show the 10% and 90% percentile and 25-75% quartile
709 of the measurements, respectively. (*) and (**) show the significance at 0.05 and 0.01 levels (*t*
710 test), respectively.

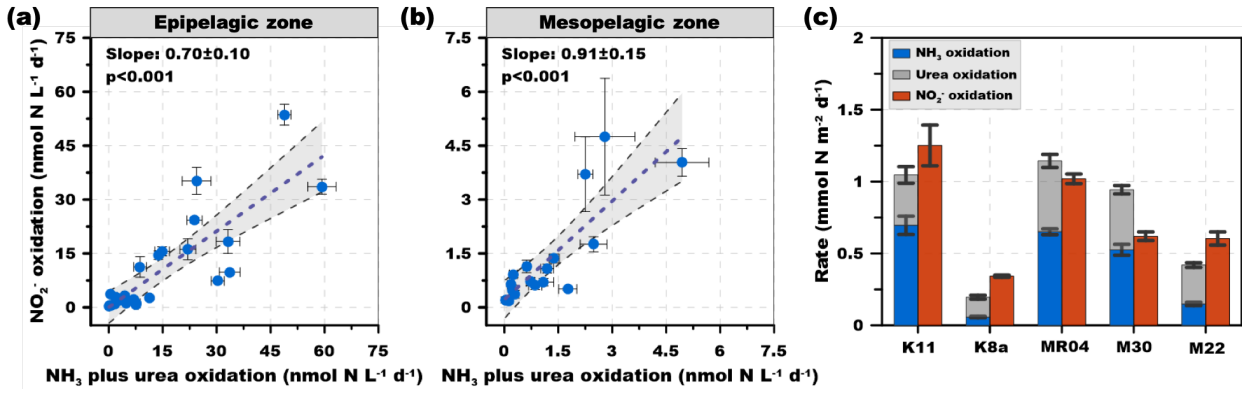

Fig. 7 Comparison of NO_2^- production and consumption rates during nitrification. (a-b) Nitrite oxidation rate versus ammonia oxidation plus urea oxidation rate in the epipelagic zone and the mesopelagic zone, respectively. (c) Comparison of the depth-integrated (0-1000 m) rates of ammonia oxidation, urea oxidation and nitrite oxidation. Note the urea oxidation rate is added to the ammonia oxidation rate in panel c. The error bars in panels a and b depict one standard deviation of triplicate rate measurements; in some cases, the error bars are smaller than the symbols. The black dashed line and grey shadow in panels a and b show linear regressions and the 95% confidence intervals, respectively. The error bars in panel c are the propagated standard deviation of the rates derived from triplicate incubations.

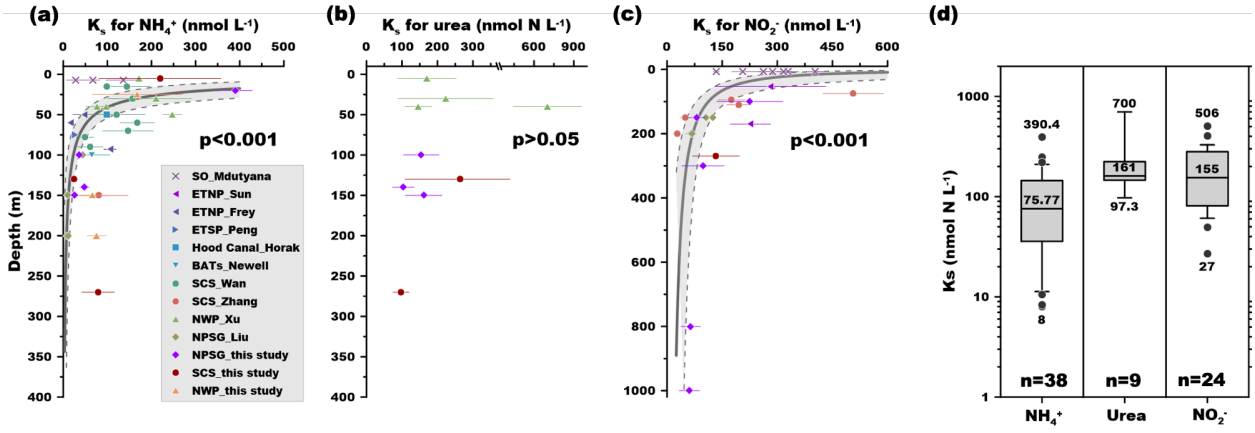

Fig. 8 Vertical distribution and statistics of the K_s of ammonia, urea, and nitrite oxidation measured in the marine systems. (a-c) The compiled K_s for NH_{4+}, urea, and NO_{2-}, respectively. The solid lines represent the power law fitting curve (insignificant for K_s for urea). (d) Statistics of the K_s values. The numbers in the box plots show the minimum, median, and maximum value, whiskers and boxes show the 10% and 90% percentile and 25-75% quartile of the measurements,

727 respectively. The data sources are from the Sothern Ocean (SO) (Mdutyana et al., 2022a, b), the
728 Eastern Tropical North Pacific (ETNP) (Frey et al., 2022; Sun et al., 2017), Eastern Tropical South
729 Pacific (ETSP) (Peng et al., 2016), the Hood Canal (Horak et al., 2013), BATs (Newell et al.,
730 2013), the South China Sea (SCS) (Wan et al., 2018; Zhang et al., 2020), the Northwestern Pacific
731 (NWP) (Xu et al., 2019), the North Pacific Subtropical Gyre (NPSG) (Liu et al., 2023), and the
732 results from this study.

733 **Table**

734 **Table 1 Depth-integrated (0-1000m) inventory of nitrogen nutrient and rates of the three**
735 **measured processes.**

	Q40	A5	K11	K8a	MR04	M30	M22
Water column inventory (0-1000m, mmol m^{-2} for NH_4^+, Urea and NO_2^-; mol m^{-2} for NO_3^-)							
NH_4^+	17.0	20.1	5.2	3.5	8.3	5.6	6.5
Urea	55.4	73.9	59.6	66.1	57.2	44.5	49.4
NO_2	15.2	25.2	18.3	12.5	17.8	11.7	13.6
NO_3	15.4	29.5	28.2	34.8	29.5	27.4	41.3
Depth-integrated rate (0-1000m, mmol N m^{-2} d^{-1})							
Ammonia oxidation	3.50±0.29	1.87±0.14	0.70±0.06	0.06±0.01	0.65±0.02	0.53±0.04	0.15±0.01
Urea oxidation	2.15±0.17	1.03±0.06	0.35±0.06	0.14±0.01	0.49±0.05	0.42±0.03	0.27±0.02
Nitrite oxidation	ND	ND	1.25±0.15	0.34±0.01	1.02±0.03	0.62±0.03	0.60±0.05

736 ND: nitrite oxidation rate was not measured at stations Q40 and A5.

737

738 **Acknowledgments**

739 We greatly appreciate the help of W. Zhang and Q. Wu during the research cruise to the
740 Northwestern Pacific; and B. Zou for collecting the samples during the South China Sea cruise.
741 We also thank T. Huang for the on-board measurement of NH_4^+, Z. Yuan, Y. Wu for NO_3^- and
742 NO_2^- measurements, L. Chen for urea measurements. We are grateful for the crew of the R/V
743 *Dongfanghong II* and R/V *Tan Kah Kee* for the onboard assistance and providing the CTD data.
744 This work was supported by the National Natural Science Foundation of China through grants
745 41890802, 92058204, 41721005 and 41849905. XSW and BBW acknowledge funding from the
746 Simons Foundation through award No. 675459 to BBW.

747 **Conflict of Interest**

748 The authors declare no competing interests.

Author contributions

Conceptualization: X. S. Wan, B. B. Ward

Data curation: X. S. Wan, M. Dai, S. J. Kao, B. B. Ward

Formal Analysis: X. S. Wan, H. Sheng, W. Q., B. B. Ward

Funding acquisition: M. Dai, S. J. Kao, B. B. Ward

Investigation: X. S. Wan, H. Sheng, H. Shen, W. Zou, J. M. Tang

Methodology: X. S. Wan, H. Sheng, H. Shen, W. Zou, J. M. Tang

Resources: M. Dai, S. J. Kao, B. B. Ward

Validation: X. S. Wan, H. Sheng, W. Q., M. Dai, S. J. Kao, B. B. Ward

Visualization: X. S. Wan, H. Sheng

Writing: original draft: X. S. Wan, B. B. Ward

Writing: review & editing: All authors

Reference

Alonso-Sáeza, L., Waller, A. S., Mende, D. R., Bakker, K., Farnelid, H., Yager, P. L., Lovejoy, C., Tremblay, J., Potvin, M., Heinrich, F., Estrada, M., Riemann, L., Bork, P., Pedrós-Alió, C. & Bertilsson, S. (2012). Role for urea in nitrification by polar marine Archaea. *Proceedings of the National Academy of Sciences*, **109,** 17989-17994. https://doi.org/10.1073/pnas.1201914109

Bayer, B., Vojvoda, J., Offre. P., Alves, R. JE., Elisabeth, N. H., Garcia, J. AL., Volland, J., Srivastava, A., Schleper, C. & Herndl, G. J. (2016). Physiological and genomic characterization of two novel marine thaumarchaeal strains indicates niche differentiation. *The ISME Journal,* **10,** 1051-1063. https://doi.org/10.1038/ismej.2015.200

Carini, P. Dupont, C. L. & Santoro, A. E. (2018). Patterns of thaumarchaeal gene expression in culture and diverse marine environments. *Environmental Microbiology,* **20,** 2112-2124. https://doi.org/10.1111/1462-2920.14107

Casciotti, K. L. (2016). Nitrite isotopes as tracers of marine N cycle processes. *Philosophical Transactions of the Royal Society A: Mathematical, Physical and Engineering Sciences,* **374,** 20150295. http://dx.doi.org/10.1098/rsta.2015.0295

777 Chen, L., Ma, J., Huang, Y., Dai, M. & Li, X. (2015). Optimization of a colorimetric method to
778 determine trace urea in seawater. *Limnology & Oceanography: Methods,* **13,** 303-311.
779 https://doi.org/10.1002/lom3.10026
780 Dai, M, Luo, Y. W., Achterberg, E. P., Browning, T. J., Cai, Y., Cao, Z., Chai, F., Chen, B.,
781 Church, M. J., Ci, D., Du, C., Gao, K., Guo, X., Hu, Z., Kao, S. J., Laws, E. A., Lee, Z.,
782 Lin, H., Liu, Q.., Liu, X., Luo, W., Meng, F., Shang, S., Shi, D., Saito, H., Song, L., Wan,
783 X. S., Wang, Y., Wang, W. L., Wen, Z., Xiu, X., Zhang, J., Zhang, R. & Zhou, K (2023).
784 Upper Ocean Biogeochemistry of Oligotrophic Subtropical Gyres: from Nutrient Sources
785 to Carbon Export. *Review of Geophysics,* **61,** e2022RG000800.
786 https://doi.org/10.1029/2022RG000800
787 Damashek, J., Tolar, B. B., Liu, Q., Okotie-Oyekan, A. O., Wallsgrove, N. J., Popp, B. N. &
788 Hollibaugh, J. T. (2019). Microbial oxidation of nitrogen supplied as selected organic
789 nitrogen compounds in the South Atlantic Bight. *Limnology and Oceanography,* **64,** 982-
790 995. https://doi.org/10.1002/lno.11089
791 Francis, C.A., Roberts, K.J., Beman, J.M., Santoro, A.E. & Oakley, B.B. (2005). Ubiquity and
792 diversity of ammoniaoxidizing archaea in water columns and sediments of the ocean.
793 *Proceedings of the National Academy of Sciences of the United States of America,* **102,**
794 14683-14688. https://doi.org/10.1073/pnas.0506625102
795 Frey, C., Sun, X., Szemberski, L., Casciotti, K. L., Garcia-Robledo, E., Jayakumar, A., Kelly, C.
796 L., Lehmann, M. F. & Ward, B. B. (2022). Kinetics of nitrous oxide production from
797 ammonia oxidation in the Eastern Tropical North Pacific. *Limnology and Oceanography,*
798 **68,** 424-438. https://doi.org/10.1002/lno.12283
799 Granger, J. & Sigman, D. M. (2009). Removal of nitrite with sulfamic acid for nitrate N and O
800 isotope analysis with the denitrifier method. *Rapid Communications in Mass Spectrometry,*
801 **23,** 3753-3762. https://doi.org/10.1002/rcm.4307
802 Gruber, N. (2008). The marine nitrogen cycle: overview and challenges. In Capone, D. G.,
803 Bronk, D. A., Mulholland, M. R. & Carpenter, E. J. (Eds.) *Nitrogen in the Marine*
804 Environment (pp. 1-50). Elsevier, Amsterdam, ed. 2.
805 Herndl, G. J. & Reinthaler, T. (2013). Microbial control of the dark end of the biological pump.
806 *Nature Geoscience,* **6,** 718-724. https://doi.org/10.1038/ngeo1921

807 Horak, R. E. A., Qin, W., Schauer, A. J., Armbrust, E. V., Ingalls, A. E., Moffett, J. W., Stahl, D.
808 A. & Devol, Allan H. (2013). Ammonia oxidation kinetics and temperature sensitivity of a
809 natural marine community dominated by Archaea. *The ISME Journal,* **7,** 2023-2033.
810 https://doi.org/10.1038/ismej.2013.75
811 Irwin, A. J., & Oliver, M. J. (2009). Are ocean deserts getting larger? *Geophysical Research*
812 *Letters*, **36,** L18609. https://doi. org/10.1029/2009gl039883
813 Ji, Q., Buitenhuis, E., Suntharalingam, P., Sarmiento, J. L. & Ward, B. B. (2018). Global nitrous
814 oxide production determined by oxygen sensitivity of nitrification and denitrification.
815 *Global Biogeochemical Cycles,* **32,** 1790-1802. https://doi.org/10.1029/2018gb005887
816 Jung, M. Y., Sedlacek, C. J., Kits, K. D., Mueller, A. J., Rhee, S. K., Hink, L., Nicol, G. W.,
817 Bayer, B., Lehtovirta-Morley, L., Wright, C., de la Torre, J. R., Herbold, C. W., Pjevac, P.,
818 Daims, H. & Wagner, M. (2022). Ammonia-oxidizing archaea possess a wide range of
819 cellular ammonia affinities. *The ISME Journal,* **16,** 272-283.
820 https://doi.org/10.1038/s41396-021-01064-z
821 Karl, D. M. & Church, M. J. (2014). Microbial oceanography and the Hawaii Ocean Time-series
822 programme. *Nature Review Microbiology,* **12,** 699-713.
823 https://doi.org/10.1038/nrmicro3333
824 Karner, K. B., DeLong, E. F. & Karl, D. M. (2001). Archaeal dominance in the mesopelagic
825 zone of the Pacific Ocean. *Nature,* **409,** 507-510. https://doi.org/10.1038/35054051
826 Kitzinger, K., Padilla, C. C., Marchant, H. K., Hach, P. F., Herbold, C. W., Kidane, A. T.,
827 Könneke, M., Littmann, S., Mooshammer, M., Niggemann, J., Petrov, S., Richter, A.,
828 Stewart, F. J., Wagner, M., Kuypers, M. M. M. & Bristow, L. A. (2019). Cyanate and urea
829 are substrates for nitrification by Thaumarchaeota in the marine environment. *Nature*
830 *Microbiology,* **4,** 234-243. https://doi.org/10.1038/s41564-018-0316-2
831 Koch, H., Lücker, S., Albertsen, M., Kitzinger, K., Herbold, C., Spieck, E., Nielsen, P. H.,
832 Wagner, M. & Daims, H. (2015). Expanded metabolic versatility of ubiquitous nitrite-
833 oxidizing bacteria from the genus *Nitrospira*. *Proceedings of the National Academy of*
834 *Sciences*, **112,** 11371-11376. https://doi.org/10.1073/pnas.1506533112
835 König, D., Conway, T. M., Ellwood, M. J., Homoky, W. B. & Tagliabue, A. (2021). Constraints
836 on the cycling of iron isotopes from a global ocean model. *Global Biogeochemical Cycles,*
837 **35,** e2021GB006968. https://doi.org/10.1029/2021gb006968

838 Laperriere, S. M., Morando, M., Capone, D. G., Gunderson, T., Smith, J. M. & Santoro, A. E.
839 (2021). Nitrification and nitrous oxide dynamics in the Southern California Bight.
840 *Limnology and Oceanography,* **66,** 1099-1112. https://doi.org/10.1002/lno.11667
841 Liu, L., Chen, M., Wan, X. S., Du, C., Liu, Z., Hu, Z., Jiang, Z. P., Zhou, K., Lin, H., Shen, H.,
842 Zhao, D., Yuan, L., Hou, L., Yang, J. Y. T., Li, X., Kao, S. J., Zakem, E. J., Qin, W., Dai,
843 M. & Zhang, Y (2023). Reduced primary nitrite maximum by cyclonic eddies in the
844 northwest Pacific subtropical gyre. *Science Advances.* **9,** eade2078.
845 https://doi:10.1126/sciadv.ade2078
846 Liu, L., Liu, M., Jiang, Y., Lin, W. & Luo, J (2021). Production and excretion of polyamines to
847 tolerate high ammonia, a case study on soil Ammonia-Oxidizing Archaeon "*Candidatus*
848 Nitrosocosmicus agrestis". *mSystems,* **6,** e01003-20. https://doi.org/10.1128/
849 mSystems.01003-20.
850 Liu, Q., Nishibori, N. & Hollibaugh, James T. (2022). Sources of polyamines in coastal waters
851 and their links to phytoplankton. *Marine Chemistry,* **242,** 104121.
852 https://doi.org/10.1016/j.marchem.2022.104121
853 Lu, X., Zou, L., Clevinger, C., Liu, Q., Hollibaugh, J. T. & Mou, X. (2014). Temporal dynamics
854 and depth variations of dissolved free amino acids and polyamines in coastal seawater
855 determined by high-performance liquid chromatography. *Marine Chemistry,* **163,** 36–44.
856 https://doi.org/10.1016/j.marchem.
857 Martens-Habbena, W., Berube, P. M., Urakawa, H., de la Torre, J. R. & Stahl, D. A. (2009).
858 Ammonia oxidation kinetics determine niche separation of nitrifying Archaea and Bacteria.
859 *Nature,* **461,** 976-979. https://doi.org/10.1038/nature08465
860 Mcllvin, M. R. & Altabet, M. A. (2005). Chemical conversion of nitrate and nitrite to nitrous
861 oxide for nitrogen and oxygen isotopic analysis in freshwater and seawater. *Analytical*
862 *Chemistry,* **77,** 5589-5595. https://doi.org/10.1021/ac050528s
863 Mdutyana, M., Marshall, T., Sun, X., Burger, J. M., Thomalla, S. J., Ward, B. B. & Fawcett, S.
864 E. (2022a). Controls on nitrite oxidation in the upper Southern Ocean: insights from winter
865 kinetics experiments in the Indian sector. *Biogeosciences,* **19,** 3425-3444.
866 https://doi.org/10.5194/bg-19-3425-2022
867 Mdutyana, M., Sun, X., Burger, J. M., Flynn, R. F., Smith, S., Horsten, N. R., Roychoudhury, A.
868 N., Planquette, H., Bucciarelli, E., Thomalla, S. J., Ward, B. B. & Fawcett, S. E. (2022b).

The kinetics of ammonium uptake and oxidation across the Southern Ocean. *Limnology and Oceanography,* **67,** 973-991. https://doi.org/10.1002/lno.12050

Newell, S. E, Fawcett, S. E. & Ward, B. B. (2013). Depth distribution of ammonia oxidation rates and ammonia-oxidizer community composition in the Sargasso Sea. *Limnology and Oceanography,* **58,** 1491-1500. https://doi.org/10.4319/lo.2013.58.4.1491

Palatinszky, M., Herbold, C., Jehmlich, N., Pogoda, M., Han, P., von Bergen, M., Lagkouvardos, I., Karst, S. M., Galushko, A., Koch, H., Berry, D., Daims, H. & Wagner, M. (2015). Cyanate as an energy source for nitrifiers. *Nature,* **524,** 105-108. https://doi.org/10.1038/nature14856

Peng, X. F., Fuchsman, C. A., Jayakumar, A., Warner, M. J., Devol, A. H. & Ward, B. B. (2016). Revisiting nitrification in the Eastern Tropical South Pacific: A focus on controls. *Journal of Geophysical Research-Oceans,* **121,** 1667-1684. https://doi.org/10.1002/2015jc011455

Pèrez, M. T., Pausz, C. & Herndl, G. J. (2003). Major shift in bacterioplankton utilization of enantiomeric amino acids between surface waters and the ocean's interior. *Limnology and Oceanography,* **48,** 755-763. https://doi.org/10.4319/lo.2003.48.2.0755

Polovina, J. J., Howell, E. A., & Abecassis, M. (2008). Ocean's least productive waters are expanding. *Geophysical Research Letters*, 35, L03618. https://doi.org/10.1029/2007gl031745

Qin, W., Wei, S. P., Zheng, Y., Choi, E., Li, X., Johnston, J., Wan, X., Abrahamson, J. B., Flinkstrom, Z., Wang, B., Li, H., Hou, L., Sun, X., Wells, M., Ngo, L., Hunt, K., Urakawa, h., Tao, X., Wang, D., Wang, D., Pan, C., Weber, P. K., Jiang, J., Zhou, J., Zhang, Y., Stahl, D. A., Ward, B. B., Mayali, X., Martens-Habbena, W. & Winkler, M. (2024). Ammonia-oxidizing bacteria and archaea exhibit differential nitrogen source preferences. *Nature Microbiology,* **9,** 524-536. https://doi.org/10.1038/s41564-023-01593-7

Qin, W., Zheng, Y., Zhao, F., Wang, Y., Urakawa, H., Martens-Habbena, W., Liu, H., Huang, X., Zhang, X., Nakagawa, T., Mende, D. R., Bollmann, A., Wang, B., Zhang, Y., Amin, S. A., Nielsen, J. L., Mori, K., Takahashi, R., Virginia Armbrust, E., Winkler, M. K. H., DeLong, E. F., Li, M., Lee, P. H., Zhou, J., Zhang, C., Zhang, T., Stahl, D. A. & Ingalls, A. E. (2020). Alternative strategies of nutrient acquisition and energy conservation map to the biogeography of marine ammonia-oxidizing archaea. *The ISME Journal,* **14,** 2595-2609. https://doi.org/10.1038/s41396-020-0710-7

900 Richon, C. & Tagliabue, A. (2019). Insights into the major processes driving the global
901 distribution of copper in the ocean from a global model. *Global Biogeochemical Cycles,*
902 **33,** 1594-1610. https://doi.org/10.1029/2019GB006280
903 Santoro, A. E., Richter, R. A. & Dupont, C. L. (2019). Planktonic marine archaea. *Annual*
904 *Review of Marine Science,* **11,** 131-158. https://doi.org/10.1146/annurev-marine-121916-
905 063141
906 Santoro, A. E., Saito, M. A., Goepfert, T. J., Lamborg, C. H., Dupont, C. L. & DiTullio,
907 Giacomo R. (2017). Thaumarchaeal ecotype distributions across the equatorial Pacific
908 Ocean and their potential roles in nitrification and sinking flux attenuation. *Limnology and*
909 *Oceanography,* **62,** 1984-2003. https://doi.org/10.1002/lno.10547
910 Shiozaki, T., Furuya, K., Kurotori, H., Kodama, T., Takeda, S., Endoh, T., Yoshikawa, Y.,
911 Ishizaka, J. & Matsuno, T. (2011). Imbalance between vertical nitrate flux and nitrate
912 assimilation on a continental shelf: Implications of nitrification. *Journal of Geophysical*
913 *Research: Oceans,* **116,** C10031. https://doi.org/10.1029/2010JC006934
914 Shiozaki, T., Hashihama, F., Endo, H., Ijichi, M., Takeda, N., Makabe, A., Fujiwara, A.,
915 Nishino, S. & Harada, N. (2021). Assimilation and oxidation of urea-derived nitrogen in
916 the summer Arctic Ocean. *Limnology and Oceanography,* **66,** 4159-4170.
917 https://doi.org/10.1002/lno.11950
918 Shiozaki, T., Ijichi, M., Isobe, K., Hashihama, F., Nakamura, K. I., Ehama, M., Hayashizaki, K.
919 I., Takahashi, K., Hamasaki, K. & Furuya, K. (2016). Nitrification and its influence on
920 biogeochemical cycles from the equatorial Pacific to the Arctic Ocean. *The ISME Journal,*
921 **10,** 2184-2197. https://doi.org/10.1038/ismej.2016.18
922 Sipler, R. E. & Bronk, D. A. (2015). Dynamics of dissolved organic nitrogen. In Hansell, D. A.
923 & Carlson, C. A. (Eds.) *Biogeochemistry of marine dissolved organic matter* (pp. 127-232).
924 Academic Press, Boston, ed. 2. https://doi.org/10.1016/B978-0-12-405940-5.00004-2
925 Smith, J. M., Damashek, J., Chavez, F. P. & Francis, C. A. (2016). Factors influencing
926 nitrification rates and the abundance and transcriptional activity of ammonia-oxidizing
927 microorganisms in the dark northeast Pacific Ocean. *Limnology and Oceanography,* **61,**
928 596-609. https://doi.org/10.1002/lno.10235

929 Sun, X., Ji, Q., Jayakumar, A. & Ward, B. B. (2017). Dependence of nitrite oxidation on nitrite
930 and oxygen in low-oxygen seawater. *Geophysical Research Lettters,* **44,** 7883-7891.
931 https://doi.org/10.1002/2017GL074355
932 Suttle, C. A., Chan, A. M. & Fuhrman, J. A. (1991). Dissolved free amino acids in the Sargasso
933 Sea: uptake and respiration rates, turnover times, and concentrations. Marine Ecology
934 Progress Series, 70, 189-199. https://doi.org/10.3354/meps070189
935 Tang, J. M., Xu, M. N., Lin,Y., Chen,H., Jin,H., Han, L. L., Zou,W. & Kao, S. J. (2022). The
936 biological transformation of ammonium and urea in a eutrophic estuarine system in
937 Southern China. *Frontiers in Marine Science,* **9,** 1040554.
938 https://doi.org/10.3389/fmars.2022.1040554
939 Tang, W., Tracey, J. C., Carroll, L., Wallace, E., Lee, J. A., Nathan, L., Sun, X., Jayakumar, A.
940 & Ward, B. B. (2022). Nitrous oxide production in the Chesapeake Bay. *Limnology and*
941 *Oceanography,* **67,** 2101-2116. https://doi.org/10.1002/lno.12191
942 Tang, W., Ward, B. B., Beman, M., Bristow, L., Clark, D., Fawcett, S., Frey, C., Fripiat, F.,
943 Herndl, G. J., Mdutyana, M., Paulot, F., Peng, X., Santoro, A. E., Shiozaki, T., Sintes, E.,
944 Stock, C., Sun, X., Wan, X. S., Xu, M. N. & Zhang, Y. (2023). Database of nitrification
945 and nitrifiers in the global ocean, *Earth System Science Data Discussion,*
946 https://doi.org/10.5194/essd-2023-194.
947 Tolar, B. B., Wallsgrove, N. J., Popp, B. N. & Hollibaugh, J. T. (2017). Oxidation of urea-
948 derived nitrogen by thaumarchaeota-dominated marine nitrifying communities.
949 *Environmental Microbiology,* **19,** 4838-4850. https://doi.org/10.1111/1462-2920.13457
950 Wan, X. S., Hou, L., Kao, S. J., Zhang, Y., Sheng, H. X., Shen, H., Tong, S., Qin, W. & Ward,
951 B. B. (2023). Pathways of N_2O production by marine ammonia-oxidizing archaea
952 determined from dual isotope labeling. *Proceedings of the National Academy of Sciences of*
953 *the United States of America,* **120,** e2220697120. https://doi:10.1073/pnas.2220697120
954 Wan, X. S., Sheng, H. X., Dai, M., Church, M. J., Zou, W., Li, X., Hutchins, D. A., Ward, B. B.
955 & Kao, S.J. (2021). Phytoplankton-nitrifier interactions control the geographic distribution
956 of nitrite in the upper ocean. *Global Biogeochemical Cycles,* **35,** e2021GB007072.
957 https://doi.org/10.1029/2021GB007072
958 Wan, X. S., Sheng, H. X., Dai, M., Zhang, Y., Shi, D., Trull, T. W., Zhu, Y., Lomas, M. W. &
959 Kao, S. J. (2018). Ambient nitrate switches the ammonium consumption pathway in the

960 euphotic ocean. *Nature Communications,* **9**, 915. https://doi.org/10.1038/s41467-018-
961 03363-0
962 Ward, B. B. (2008). Nitrification in marine systems. In Capone, D. G., Bronk, D. A.,
963 Mulholland, M. R. & Carpenter, E. J. (Eds.) *Nitrogen in the Marine* Environment (pp. 199-
964 261). Elsevier, Amsterdam, ed. 2.
965 Ward, B. B. & Zafiriou, O. C. (1988). Nitrification and nitric oxide in the oxygen minimum of
966 the eastern tropical North Pacific. *Deep Sea Research Part A. Oceanographic Research*
967 *Papers*, **35,** 1127-1142. http://dx.doi.org/10.1016/0198-0149(88)90005-2
968 Weigand, M. A., Foriel, J., Barnett, B., Oleynik, S. & Sigman, D. M. (2016). Updates to
969 instrumentation and protocols for isotopic analysis of nitrate by the denitrifier method.
970 *Rapid Communications in Mass Spectrometry,* **30,** 1365-1383.
971 https://doi.org/10.1002/rcm.7570
972 Widner, B., Fuchsman, C. A., Chang, B. X., Rocap, G. & Mulholland, M. R. (2018). Utilization
973 of urea and cyanate in waters overlying and within the eastern tropical north Pacific oxygen
974 deficient zone. *FEMS Microbiology Ecology,* **94,** FIY138.
975 https://doi.org/10.1093/femsec/fiy138
976 Widner, B., Mulholland, M. R. & Mopper, K. (2016). Distribution, sources, and sinks of cyanate
977 in the coastal North Atlantic Ocean. *Environmental Science & Technology Letters,* **3,** 297-
978 302. https://doi.org/10.1021/acs.estlett.6b00165
979 Xu, M. N., Li, X., Shi, D., Zhang, Y., Dai, M., Huang, T., Glibert, P. M. & Kao, S. J. (2019).
980 Coupled effect of substrate and light on assimilation and oxidation of regenerated nitrogen
981 in the euphotic ocean. *Limnology& Oceanography,* **64,** 1270-1283.
982 https://doi.org/10.1002/lno.11114
983 Zakem, E. J., Al-Haj, A., Church, M. J., van Dijken, G. L., Dutkiewicz, S., Foster, S. Q.,
984 Fulweiler, R. W., Mills, M. M. & Follows, M. J. (2018). Ecological control of nitrite in the
985 upper ocean. *Nature Communications,* **9,** 1206. http://doi: 10.1038/s41467-018-03553-w
986 Zhang, J. Z. (2000). Shipboard automated determination of trace concentrations of nitrite and
987 nitrate in oligotrophic water by gas-segmented continuous flow analysis with a liquid
988 waveguide capillary flow cell. *Deep Sea Research Part I: Oceanographic Research*
989 *Papers,* **47,** 1157-1171.

990 Zhang, Y., Qin, W., Hou, L., Zakem, E. J., Wan, X., Zhao, Z., Liu, L., Hunt, K. A., Jiao, N.,
991 Kao, S. J., Tang, K., Xie, X., Shen, J., Li, Y., Chen, M., Dai, X., Liu, C., Deng, W., Dai,
992 M., Ingalls, A. E., Stahl, D. A. & Herndl, G. J. (2020). Nitrifier adaptation to low energy
993 flux controls inventory of reduced nitrogen in the dark ocean. *Proceedings of the National*
994 *Academy of Sciences*, **117,** 4823-4830. https://doi.org/10.1073/pnas.1912367117
995 Zhu, Y., Sun, J., Wang, Y., Li, S., Xu, T., Wei, Z. & Qu, T. (2019). Overview of the multi-layer
996 circulation in the South China Sea. *Progress in Oceanography,* **175,** 171-182.
997 https://doi.org/10.1016/j.pocean.2019.04.001
998 Zhu, Y., Yuan, D., Huang, Y., Ma, J. & Feng, S. (2013). A sensitive flow-batch system for on
999 board determination of ultra-trace ammonium in seawater: Method development and
1000 shipboard application. *Analytica Chimica Acta,* **794,** 47-54.
1001 http://dx.doi.org/10.1016/j.aca.2013.08.009
1002
1003